A hybrid kinetic-fluid model for solving the gas dynamics Boltzmann-BGK equation

Nicolas Crouseilles, Pierre Degond, Mohammed Lemou

A hybrid kinetic-fluid model for solving the gas dynamics Boltzmann-BGK equation.

N. Crouseilles [a, b], P. Degond [a], and M. Lemou [a]

[a] MIP, UMR CNRS 5640, UFR MIG, Université Paul Sabatier
118, route de Narbonne, 31062 Toulouse cedex, France
email: degond@mip.ups-tlse.fr, lemou@mip.ups-tlse.fr

[b] CEA-CESTA (DEV/SIS), BP2 33114 Le Barp, France
email: crouseilles@mip.ups-tlse.fr

Abstract

Our purpose is to derive a hybrid model for particle systems which combines a kinetic description of the fast particles with a fluid description of the thermal ones. In the present work, fast particles will be described through a collisional kinetic equation of Boltzmann-BGK type while thermal particles will be modeled by means of a system of Euler type equations. Then, we construct a numerical scheme for this model. This scheme satisfies exact conservation properties. We validate the approach by presenting various numerical tests.

Key words: BGK equation, Euler equations, entropy minimization principle, kinetic-hydrodynamic coupling, numerical schemes.

1 Introduction:

In rarefied gas dynamics, for strongly non-equilibrium situations, fluid models are inappropriate and one must resort to a kinetic description such as that provided by the Boltzmann equation. But the cost of the numerical resolution of this model is very prohibitive in terms of both CPU time and memory storage. We refer the reader to [4], [26], [2], ... In the present work, we propose a hybrid kinetic/fluid model describing the evolution of slow (or thermal) particles by means of a fluid model, and restricting the use of the kinetic model to the modeling of fast (or suprathermal) particles.

Fluid dynamical descriptions are based on the assumption that the mean free path of a particle is very small compared to the typical macroscopic length. In this case, the distribution function of the particles approaches a local equilibrium represented by a maxwellian, the parameters of which are the fluid variables (density, mean velocity and temperature). The evolution of the fluid variables is governed by the Euler or Navier-Stokes equations. More precisely, if τ is

the Knudsen number (ratio of the particle mean free path to the typical macroscopic scale), an expansion of the solution of the Boltzmann equation in power of τ can be performed (Hilbert or Chapman-Enskog expansion [9], [8]). At the leading order in τ, the distribution function is approximated by a maxwellian whose parameters obey the Euler equations. If the next order is retained, the fluid parameters solve the compressible Navier-Stokes equations, where the diffusion terms (viscosity and heat conductivity) are of the order of τ. When τ is small without being very small, the Navier-Stokes equations offer a quite good compromise between physical accuracy and numerical efficiency. However, when τ becomes larger, the Navier-Stokes equations break down, as well as any model attempting to take into account higher order powers in τ (like *e.g.* the Burnett equations).

Our model is aimed at transition regimes, where $\tau = O(1)$, when the Navier-Stokes equations surely break down. In such a situation, one must resort to the resolution of the full kinetic equation.

Solving a kinetic equation requires the discretization of large number of variables (3 dimensions in position, 3 dimensions in velocity plus the time). Moreover, a kinetic equation very often involves stiff terms in the collision operator and its computational cost is often quite expensive. To overcome these problems, probably the most efficient method is the Monte-Carlo method ([4], [26], [18], ...). Some deterministic methods ([15], [29], [7], [22], ...) have been recently developped with some success. Nevertheless, the search for models which would give a good approximation of the physics at a reasonable computer cost is still not complete. Our work is a contribution in this direction. It partly relies on Levermore's entropy minimization approach (see [21]), which was used to develop higher order moment hierachies, in the spirit of earlier work by Grad ([16], [17]) or Müller and Ruggeri (see [25]). Related approches can be also be found in [14] where half moment expansions are used.

In this paper, we present a hybrid kinetic/fluid model based on a domain decomposition method in the velocity variable. In order to simplify the presentation, we consider a Bathnagar-Gross-Krook (BGK) model (instead of the full Boltzmann operator) as a starting point (see [3]). The unknown distribution function $f = f(t, x, v)$ depends on time $t \geq 0$, on space $x \in \mathbb{R}^d$, and on velocity $v \in \mathbb{R}^d, d = 1, 2, 3$, and solves

$$\frac{\partial f}{\partial t} + v \cdot \nabla_x f = \frac{1}{\tau}(\mathcal{M}_{[f]} - f). \tag{1.1}$$

$\mathcal{M}_{[f]}$ is the maxwellian with the same moments as f, *i.e.*

$$\mathcal{M}_{[f]}(v) = \frac{n}{(2\pi T)^{\frac{d}{2}}} \exp\left[-\frac{|v-u|^2}{2T}\right] \tag{1.2}$$

where n, u, T (the density, mean velocity and temperature) satisfy:

$$\begin{aligned} n &= \int_{\mathbb{R}^d} f(v)dv, \\ nu &= \int_{\mathbb{R}^d} vf(v)dv, \\ dnT &= \int_{\mathbb{R}^d} |v-u|^2 f(v)dv. \end{aligned} \tag{1.3}$$

In other words, $\mathcal{M}_{[f]}$ is defined as the only maxwellian whose parameters n, u, T are such that:

$$\int_{\mathbb{R}^d} f(v) \begin{pmatrix} 1 \\ v \\ |v|^2 \end{pmatrix} dv = \int_{\mathbb{R}^d} \mathcal{M}_{[f]}(v) \begin{pmatrix} 1 \\ v \\ |v|^2 \end{pmatrix} dv. \tag{1.4}$$

Finally, $\tau > 0$ represents a scaled relaxation time. Equation (1.1) is written in scaled variables, the time and space scales being related to the problem under consideration (*e.g.* the domain size). Equation (1.1) is supplemented with an initial condition $f_{(t=0)} = f_0$.

Our model relies on the assumption that the particles can be clearly grouped into two categories. The first category consists of thermal particles, whose distribution function is close to a maxwellian. The second category is that of suprathermal or energetic particles. They are supposed to represent a small proportion of the total number of particles. On the other hand, their distribution function can be anything. Of course, there are situations where such an assumption is clearly untrue (for instance, the case of two interpenetrating particle beams for which the distribution function is the sum of two maxwellians of nearly equal weights), but our belief is this assumption is satisfied in many cases of practical interest. We shall give some examples later on. Following this assumption, we choose a domain B_1 in velocity space (most often a ball centered in $\underline{u}$ and with radius $\mathcal{R}\sqrt{\underline{T}}$, where $\underline{u}$ and $\underline{T}$ are a velocity and a temperature to be conveniently chosen, and $\mathcal{R}$ is a fixed number). We suppose that the particle distribution function can be approximated by a maxwellian inside B_1. Therefore, we make the Ansatz that the solution of (1.1) can be approximated by:

$$f = \begin{cases} \mathcal{M}_1, & v \in B_1 \\ f_2, & v \in B_2 = \mathbb{R}^d \setminus B_1, \end{cases} \tag{1.5}$$

where $\mathcal{M}_1$ is a maxwellian. In practice, $\underline{u}$ and $\underline{T}$ are space and time dependent functions. They are chosen to be the mean velocity and the temperature of f.

Let (n_1, u_1, T_1) be the parameters of $\mathcal{M}_1$. On should note that $u_1 \neq \underline{u}$ and $T_1 \neq \underline{T}$ in general. We must derive a set of fluid equations for (n_1, u_1, T_1) from the BGK model (1.1), as well as a kinetic equation for f_2. The way we achieve this task is by taking the moment equations of (1.1) on the domain B_1. We obtain conservation equations for the mass, momentum and energy of the thermal particles *i.e.* those contained in B_1. As usual, these equations are not closed. To close the system, we use Levermore's entropy minimization strategy [21] and take the distribution function in B_1 to be the maxwellian $\mathcal{M}_1$, which minimizes the entropy of the thermal particles, subject to the constraints of given mass, momentum and energy in B_1. The so-obtained system differs from the standard Euler equations in the expression of the fluxes on the one hand (because these fluxes are integrated over B_1 only) and in the coupling with the BGK equation which describes the evolution of the distribution function f_2. This coupling is due first to the collision operator (collisions may "send" particles from B_1 to B_2 and *vice versa*), but also, to the fact that $\underline{u}$ and $\underline{T}$ are depending on (t, x). Therefore, the variations of the fluid domain in space and time induce fluxes of particles from B_1 to B_2 and *vice versa*. These fluxes appear as source and sink terms depending on f_2 in the Euler equations, and as boundary conditions depending on $\mathcal{M}_1$ at the boundary of B_2 for f_2.

We must point out how important it is for a numerical discretization to respect a perfect flux balance between the two sets of equations (the Euler equations on B_1 and the BGK equation

on B_2). Otherwise, there might exist local sources or sinks of mass, momentum and energy which is obviously unphysical.

We shall present a numerical strategy which respects this balance perfectly. It relies first on a full time, space and velocity discretization of the BGK equation by a conservative finite volume scheme. Then, the analogue of the decomposition (1.5) is performed in the discrete distribution function; the discrete moment equations are obtained for the thermal particles and a discrete entropy minimization principle is used to close the equations.

In this paper, we try to demonstrate the validity of the hybrid approach against the full kinetic equation. Therefore, we do not try to optimize the numerical efficiency and at this stage, our hybrid model is still more costly than (or at least as costly as) a direct finite volume simulation of the BGK equation. The reason is that the computation of the numerical fluxes for the Euler equations is done by discrete integration of the maxwellian on the mesh discretization of the phase space. Therefore, the storage requirements and computational complexity of the method is the same as for the resolution of the full BGK equation by a deterministic method.

Cost reduction will be obtained by two means: a faster computation of the numerical fluxes, possibly involving some pre-storage on the one hand, and a Lagrangian (particle type) discretization of the distribution function on B_2. These concepts will be developped in future work.

We now outline some similar approaches in the literature. First this approach was developped for diffusion equations in [10], and for hydrodynamics equations in [11]. It bears some similarities with the so-called δf method ([6], [27]). However, the δf approach relies on writing the distribution function as $f = \mathcal{M} + \delta f$ with $\mathcal{M}$ a maxwellian whose parameters are solutions of the standard Euler equations and δf satisfies a perturbation equation involving some approximations. Therefore, everywhere in velocity space, there is a superposition of a thermal distribution function $\mathcal{M}$ and a non-thermal part δf. The idea of using moments over sub-regions of velocity space is also present in [14]. Most hybrid kinetic/fluid approaches used so far are based on a domain-decomposition *in position space*: a fluid model is used except in specific regions where the flow is identified as being far from equilibrium, and where a kinetic model is used ([5], [24], [23], ...). Then, suitable interface conditions are set up at the kinetic/fluid interface. Sometimes, an overlap of the kinetic and fluid regions is performed.

Levermore's moment hierarchy of models [21] is sometimes used as an alternative to kinetic models. This approach has been pioneered by Grad (see [16]) and has been thoroughly investigated in the physics literature by Müller and Ruggeri (see [25]). It has been applied to rarefied gas dynamics by [19], [22], [24], semiconductor physics (see [1]), etc, ... The entropy minimization approach, which founds Levermore's approach as well as the present work has also found applications to deterministic numerical methods for the BGK equation, like *e.g.* in [22].

The paper is organized as follows: in section 2, the hybrid model is derived following the ideas outlined above. In section 3, its fully conservative numerical discretization is proposed. For the sake of simplicity, we restrict to a one-dimensional model on both space and velocity. In section 4, results of numerical simulations are presented. A few technical points are developped in appendix A, B and C.

2 Derivation of the hybrid model:

Our starting point is the Boltzmann-BGK equation (1.1)(1.2). Let us introduce some notations:

Definition 2.1. *For all function $g : \mathbb{R}^d \longrightarrow \mathbb{R}$, we define for $i = 1, 2$:*

$$g_i(v) = \begin{cases} g(v) & \text{if } v \in B_i \\ 0 & \text{otherwise,} \end{cases}$$

where B_1 is defined by $B_1 = \left\{ v \in \mathbb{R}^d \text{ s.t. } |v - \underline{u}| \leq \mathcal{R}\sqrt{\underline{T}} \right\}$ and $B_2 = \mathbb{R}^d \setminus B_1$.

Remark 2.2 *Later on, $\underline{u}$ and $\underline{T}$ will be chosen as the mean velocity and temperature of the distribution function f over $\mathbb{R}^d$.*

Our goal is to approximate (1.1)(1.2) by a fluid/kinetic model. Associated to the solution f to (1.1)(1.2), the distribution function f_2 is the unknown of the kinetic part of the hybrid model. On the other hand, the fluid part must be a closed system of $(d+2)$ equations satisfied by the moments of f_1 on B_1; they are given by $U_1 = (n_1, P_1, 2W_1)^T$ such that:

$$\int_{B_1} f_1(v) \begin{pmatrix} 1 \\ v \\ |v|^2 \end{pmatrix} dv = \begin{pmatrix} n_1 \\ P_1 \\ 2W_1 \end{pmatrix} = U_1, \tag{2.1}$$

with n_1 the density, P_1 the momentum and W_1 the total energy of f_1 on B_1. Integrating (1.1) on B_1 against the vector of conserved quantities $m(v) = (1, v, |v|^2)^T$ with respect to the velocity variable $v \in B_1$ leads to a non-closed system of equations for U_1. This is the well-known "moment closure problem" in kinetic theory. To close these equations, we shall use Levermore's strategy, based on the entropy minimization principle (see [21]). However, the present situation is different from that investigated by Levermore, in that the velocity set of integration is bounded, and the approach requires a few minor adjustments.

First, we introduce the entropy functional related to the domain B_1:

$$H_1(g) = \int_{B_1} g(v) \log(g(v)) dv, \quad \forall g \geq 0,$$

and the corresponding entropy minimization problem,

$$\begin{cases} \text{Given } n_1 \geq 0, P_1 \in \mathbb{R}^d, W_1 \geq 0, \text{ find a nonnegative function } \mathcal{M}_1 \text{ on } B_1, \\ \text{realizing the following minimum:} \\ \text{Min} \left\{ H_1(g), \ g \geq 0 \ \text{ s.t. } \ \int_{B_1} g(v) \begin{pmatrix} 1 \\ v \\ |v|^2 \end{pmatrix} dv = \begin{pmatrix} n_1 \\ P_1 \\ 2W_1 \end{pmatrix} \right\} \end{cases} \tag{2.2}$$

If (2.2) has a solution, then the system of moments U_1 derived from (1.1)(1.2) can be closed by a distribution function that coincides with that solution. This closure strategy, as pointed out by Levermore [21], ensures the hyperbolicity of the so-obtained system (here, if $\underline{u}$ and $\underline{T}$ are chosen *a priori*). The following proposition solves the entropy minimization problem (2.2) (following results in [20]):

Proposition 2.3 *The entropy minimization problem (2.2) has a solution if and only if*

$$|P_1|^2 \leq 2n_1W_1, \tag{2.3}$$

$$\frac{2n_1W_1 - |P_1|^2}{n_1^2} + |\underline{u} - \frac{P_1}{n_1}|^2 \leq \mathcal{R}^2\underline{T}. \tag{2.4}$$

Moreover, under conditions (2.3), (2.4), the solution is unique and is a maxwellian function:

$$\mathcal{M}_1(v) = \exp(\lambda^1 \cdot m(v)) = \exp(\lambda_0^1 + \lambda_1^1 \cdot v + \lambda_2^1|v|^2), \tag{2.5}$$

where $\lambda^1 = (\lambda_0^1, \lambda_1^1, \lambda_2^1)^T \in \mathbb{R}^{d+2}$ *is uniquely determined by the following relation:*

$$\int_{B_1} \exp(\lambda^1 \cdot m(v))m(v)dv = \begin{pmatrix} n_1 \\ P_1 \\ 2W_1 \end{pmatrix}, \quad \textit{with} \quad m(v) = (1, v, |v|^2)^T. \tag{2.6}$$

For the proof, we refer the reader to appendix A.

The so-obtained distribution $\mathcal{M}_1$, of the form (2.5), is used to close our moment system. We are now able to write the hybrid model. For this purpose, let us first introduce some notations. The quantities,

$$\begin{pmatrix} \psi_{n_1} \\ \psi_{P_1} \\ 2\psi_{W_1} \end{pmatrix} = \int_{B_1} \mathcal{M}_1(v)vm(v)dv = \int_{B_1} \mathcal{M}_1(v) \begin{pmatrix} v \\ v \otimes v \\ |v|^2 v \end{pmatrix} dv, \tag{2.7}$$

are the moment fluxes, with $m(v) = (1, v, |v|^2)^T$. The term,

$$\overrightarrow{F}(v) = \mathcal{D}\left(\frac{v - \underline{u}}{\mathcal{R}\sqrt{\underline{T}}}\right), \quad \text{with} \quad \mathcal{D} = \frac{\partial}{\partial t} + v \cdot \nabla_x, \tag{2.8}$$

is a force which results from the space and time variations of B_1 as we shall see later on. Now, if we denote by $\mathbb{S}(\underline{u}, \mathcal{R}\sqrt{\underline{T}})$ the boundary of B_1, which, in the case we consider, is a sphere of center $\underline{u}$ and radius $\mathcal{R}\sqrt{\underline{T}}$, we can introduce the following sets:

$$\mathbb{S}_- = \{v \in \mathbb{S}(\underline{u}, \mathcal{R}\sqrt{\underline{T}}) \ \text{ s.t. } \ \overrightarrow{F}(v) \cdot \overrightarrow{\nu} < 0\}, \tag{2.9}$$

$$\mathbb{S}_+ = \{v \in \mathbb{S}(\underline{u}, \mathcal{R}\sqrt{\underline{T}}) \ \text{ s.t. } \ \overrightarrow{F}(v) \cdot \overrightarrow{\nu} > 0\}, \tag{2.10}$$

where $\overrightarrow{\nu}$ is the outward unit normal to $\mathbb{S}(\underline{u}, \mathcal{R}\sqrt{\underline{T}})$. If $dS(v)$ is the Euclidean surface element on $\mathbb{S}(\underline{u}, \mathcal{R}\sqrt{\underline{T}})$, we can then define the following boundary outgoing and incoming semi-fluxes:

$$\begin{pmatrix} L_{n_1} \\ L_{P_1} \\ 2L_{W_1} \end{pmatrix} := \int_{\mathbb{S}_+} \overrightarrow{F}(v) \cdot \overrightarrow{\nu}\mathcal{M}_1(v)m(v)dS(v),$$

$$\begin{pmatrix} G_{n_1} \\ G_{P_1} \\ 2G_{W_1} \end{pmatrix} := \int_{\mathbb{S}_-} |\overrightarrow{F}(v) \cdot \overrightarrow{\nu}|f_2(v)m(v)dS(v),$$

(where "L" is for "loss" and "G" for "gain": we shall see that they enter as loss and gain terms in the Euler equations). If we take the moments of (1.1), make the approximation $f_1 \simeq \mathcal{M}_1$ given by (2.5) and (2.6), and if we couple the so-obtained closed system to the restriction of (1.1) to B_2 (where f_1 is again replaced by $\mathcal{M}_1$ on B_1), then we obtain the following hybrid model:

Proposition 2.4 *With the previous notations, the hybrid fluid/kinetic model of unknowns* (n_1, P_1, W_1, f_2) *is written:*

$$\begin{array}{l} \dfrac{\partial}{\partial t}\begin{pmatrix} n_1 \\ P_1 \\ W_1 \end{pmatrix} + \nabla_x \cdot \begin{pmatrix} \psi_{n_1} \\ \psi_{P_1} \\ \psi_{W_1} \end{pmatrix} = \dfrac{1}{\tau}\begin{pmatrix} n^{(1)} - n_1 \\ P^{(1)} - P_1 \\ W^{(1)} - W_1 \end{pmatrix} - \begin{pmatrix} L_{n_1} \\ L_{P_1} \\ L_{W_1} \end{pmatrix} + \begin{pmatrix} G_{n_1} \\ G_{P_1} \\ G_{W_1} \end{pmatrix}, \\ \dfrac{\partial f_2}{\partial t} + v \cdot \nabla_x f_2 = \dfrac{1}{\tau} Q_2(f_2, \mathcal{M}_1), \end{array} \tag{2.11}$$

with the following boundary conditions:

$$f_2(v) = \mathcal{M}_1(v), \quad \forall v \in \mathbb{S}_+.$$

The moments $(n_1, P_1, W_1)^T$ *are given by (2.1). Moreover, the collision term is given by:*

$$Q_2(f_2, \mathcal{M}_1) = (\mathcal{M}_{[\mathcal{M}_1+f_2],2}(v) - f_2(v)), \ v \in B_2,$$

where $\mathcal{M}_{[\mathcal{M}_1+f_2]}$ *(whose parameters are the density, mean velocity and temperature of* $\mathcal{M}_1 + f_2$*) satisfies:*

$$\int_{\mathbb{R}^d} \mathcal{M}_{[\mathcal{M}_1+f_2]}(v) m(v) dv = \int_{\mathbb{R}^d} (\mathcal{M}_1(v) + f_2(v))\, m(v) dv.$$

Moreover, we denote:

$$\begin{pmatrix} n^{(1)} \\ P^{(1)} \\ 2W^{(1)} \end{pmatrix} = \int_{B_1} \mathcal{M}_{[\mathcal{M}_1+f_2]}(v) m(v) dv,$$

with $m(v) = (1, v, |v|^2)^T$.

Remark 2.5 *Under the assumption that* $\underline{u}$ *and* $\underline{T}$ *are chosen a priori, the fluid part of the hybrid model is hyperbolic. This is a simple consequence of Levermore's result (see [21]).*

Proof. We integrate (1.1) with respect to v on B_1, after multiplication by $(1, v, |v|^2)^T$. We get:

$$\int_{B_1} \frac{\partial f}{\partial t}(v) \begin{pmatrix} 1 \\ v \\ |v|^2 \end{pmatrix} dv + \int_{B_1} v \cdot \nabla_x f(v) \begin{pmatrix} 1 \\ v \\ |v|^2 \end{pmatrix} dv = \frac{1}{\tau} \int_{B_1} (\mathcal{M}_{[f]} - f)(v) \begin{pmatrix} 1 \\ v \\ |v|^2 \end{pmatrix} dv. \tag{2.12}$$

First, we recall the notation,

$$U_i = \int_{B_i} f_i(v) \begin{pmatrix} 1 \\ v \\ |v|^2 \end{pmatrix} dv = \begin{pmatrix} n_i \\ P_i \\ 2W_i \end{pmatrix}, \ i = 1, 2, \tag{2.13}$$

for the moments of $f_i, \ i = 1, 2$, and introduce similar notations for the fluxes,

$$\varphi(f_i) = \int_{B_i} f_i(v) v \begin{pmatrix} 1 \\ v \\ |v|^2 \end{pmatrix} dv, \ i = 1, 2.$$

Let us consider the left-hand side of (2.12). If we exchange derivatives and integrals, there appear some boundary terms. To compute them, we use a change of variables that transforms B_1 into the fixed ball $B(0,1)$ of radius 1 and whose center is 0:

$$w = \frac{v - \underline{u}}{\mathcal{R}\sqrt{\underline{T}}}. \tag{2.14}$$

We then set $f_1(t,x,v) = g_1(t,x,w)$, and obtain:

$$\begin{aligned}
&\int_{B_1} \left(\frac{\partial f_1}{\partial t} + v \cdot \nabla_x f_1 \right) m(v) dv \\
&\quad = \int_{B(0,1)} \left(\frac{\partial g_1}{\partial t} + (\mathcal{R}\sqrt{\underline{T}} w + \underline{u}) \cdot \nabla_x g_1 + \overrightarrow{F_1}(w) \cdot \nabla_w g_1 \right) \tilde{m}(w) J dw \\
&\quad = \frac{\partial}{\partial t} \int_{B(0,1)} g_1 \tilde{m}(w) J dw - \int_{B(0,1)} g_1 \frac{\partial}{\partial t} (\tilde{m}(w) J) dw \\
&\qquad + \nabla_x \cdot \int_{B(0,1)} (\mathcal{R}\sqrt{\underline{T}} w + \underline{u}) g_1 \tilde{m}(w) J dw - \int_{B(0,1)} g_1 \nabla_x \cdot ((\mathcal{R}\sqrt{\underline{T}} w + \underline{u}) \tilde{m}(w) J) dw \\
&\qquad - \int_{B(0,1)} g_1 \nabla_w \cdot (\overrightarrow{F_1}(w) \tilde{m}(w) J) dw + \int_{\mathbb{S}(0,1)} \overrightarrow{F_1}(w) \cdot \overrightarrow{\nu} g_1 \tilde{m}(w) J dS(w),
\end{aligned} \tag{2.15}$$

where $\overrightarrow{\nu}$ is the outward unit normal to $B(0,1)$,

$$\overrightarrow{F_1}(w) = -\frac{1}{\mathcal{R}\sqrt{\underline{T}}} \mathcal{D}_1 \left(\mathcal{R}\sqrt{\underline{T}} w + \underline{u} \right), \quad \text{with} \quad \mathcal{D}_1 = \frac{\partial}{\partial t} + (\mathcal{R}\sqrt{\underline{T}} w + \underline{u}) \cdot \nabla_x, \tag{2.16}$$

is a force term and,

$$\tilde{m}(w) = \begin{pmatrix} 1 \\ \mathcal{R}\sqrt{\underline{T}} w + \underline{u} \\ |\mathcal{R}\sqrt{\underline{T}} w + \underline{u}|^2 \end{pmatrix}.$$

Finally,

$$J = (\mathcal{R}\sqrt{\underline{T}})^d, \quad d = 1, 2, 3,$$

is the Jacobian of the change of variables (2.14). Some calculations (which are developped in Appendix B) show that the sum of the second term, the fourth and the fifth terms of (2.15) vanishes. So, if we return to the original v variable, we obtain:

$$\begin{aligned}
\int_{B_1} \left(\frac{\partial f_1}{\partial t} + v \cdot \nabla_x f_1 \right) m(v) dv &= \frac{\partial}{\partial t} \int_{B_1} f_1 m(v) dv + \nabla_x \cdot \int_{B_1} v f_1 m(v) dv \\
&\quad + \int_{\mathbb{S}(\underline{u}, \mathcal{R}\sqrt{\underline{T}})} \overrightarrow{F}(v) \cdot \overrightarrow{\nu} f_1 m(v) dS(v),
\end{aligned} \tag{2.17}$$

where $\overrightarrow{F}(v)$ is the force (2.16) expressed in terms of v,

$$\overrightarrow{F}(v) = \mathcal{D} \left(\frac{v - \underline{u}}{\mathcal{R}\sqrt{\underline{T}}} \right), \quad \text{with} \quad \mathcal{D} = \frac{\partial}{\partial t} + v \cdot \nabla_x.$$

Now, using (2.12) and (2.17), we obtain the following moment system:

$$\frac{\partial U_1}{\partial t} + \nabla_x \cdot \varphi(f_1) = \frac{1}{\tau} \int_{B_1} \left(\mathcal{M}_{[f_1+f_2]}(v) - f_1(v) \right) m(v) dv - \int_{\mathbb{S}(\underline{u}, \mathcal{R}\sqrt{\underline{T}})} \overrightarrow{F}(v) \cdot \overrightarrow{\nu} f_1(v) m(v) dS.$$

The boundary terms represent the exchange fluxes between the kinetic and the fluid zones. We decompose these boundary terms into outgoing semi-fluxes:

$$\int_{\mathbb{S}_+} \overrightarrow{F}(v) \cdot \overrightarrow{\nu} f_1(v) m(v) dS,$$

and incoming semi-fluxes:

$$\int_{\mathbb{S}_-} |\overrightarrow{F}(v) \cdot \overrightarrow{\nu}| f_1(v) m(v) dS. \tag{2.18}$$

This last term (2.18) takes into account particles fluxes from B_2 to B_1; these fluxes are due to the variation of the ball B_1. Therefore these incoming particles are modeled by f_2 and, using the boundary conditions, (2.18) becomes:

$$\int_{\mathbb{S}_-} |\overrightarrow{F}(v) \cdot \overrightarrow{\nu}| f_2(v) m(v) dS.$$

Now, we make the approximation $f_1(v) \simeq \mathcal{M}_1(v),\ \forall v \in B_1$ where $\mathcal{M}_1$ is given by (2.5) and (2.6) (with n_1, P_1, W_1 defined by (2.13)). Then, we obtain the first part of (2.11); the coupling with the restriction of (1.1) to B_2 (where f_1 is always approximated by $\mathcal{M}_1$) leads to the hybrid model (2.11). □

3 Numerical schemes for the hybrid model:

In this section, we present a numerical scheme for the hybrid model (2.11). The main difficulty comes from the dependence of $B_1 = \left\{ v \in \mathbb{R}^d \text{ s.t. } |v - \underline{u}| \leq \mathcal{R}\sqrt{\underline{T}} \right\}$ on both time and space. As pointed out in the introduction, the variations of B_1 in position and time induce fluxes of particles from B_1 to B_2 and *vice versa*. Then the mass, momentum and energy fluxes into B_2 must be exactly balanced by the same fluxes out of B_1, otherwise unphysical source or sink terms will appear. To ensure these conservations at the discrete level, we first start from a fully discretized version of the BGK equation in position, velocity and time, and perform the domain decomposition and passage to the fluid quantities on B_1, directly on the discrete equations. The motion of the ball B_1, which takes into account the evolution of the mean velocity $\underline{u}$ and the temperature $\underline{T}$, is performed at the end of each discretization step.

For the sake of simplicity, we restrict to a one-dimensional problem in both position and velocity space, with a cartesian grid $x_i = i\Delta x,\ v_k = k\Delta v,\ i, k \in \mathbb{Z}$, while $t^n = n\Delta t$ is the time discretization, $n \in \mathbb{N}$. Like in the continuous case (see section 2), our starting point is the BGK equation. We first discretize (1.1), (1.2) on the full velocity space, following the strategy developped in [22]. We approximate $f(t^n, x_i, v_k)$ by $f_{i,k}^n$ such that:

$$f_{i,k}^{n+1} = f_{i,k}^n - v_k^+ \frac{\Delta t}{\Delta x} \left[f_{i,k}^n - f_{i-1,k}^n \right] - v_k^- \frac{\Delta t}{\Delta x} \left[f_{i+1,k}^n - f_{i,k}^n \right] + \frac{\Delta t}{\tau} \left[\mathcal{E}_{i,k}^n - f_{i,k}^n \right], \tag{3.1}$$

with $v_k^{\pm} = \frac{1}{2}(v_k \pm |v_k|)$ and where $(\mathcal{E}_{i,k}^n)_{k\in\mathbb{Z}}$ realizes the following minimum:

$$\text{Min}\left\{\sum_{k\in\mathbb{Z}} g_k \log(g_k)\Delta v,\ g_k \geq 0 \ \text{ s.t. } \ \sum_{k\in\mathbb{Z}} m_k g_k \Delta v = U_i^n\right\}, \tag{3.2}$$

with the prescribed moments $U_i^n = \sum_{k\in\mathbb{Z}} f_{i,k}^n m_k \Delta v$ and $m_k = (1, v_k, |v_k|^2)$. In [22], it is shown that the operator $(\mathcal{E}_{i,k}^n - f_{i,k}^n)$ is an approximation of the BGK operator. In particular, thanks to Theorem 3.1 of [22], $(\mathcal{E}_{i,k}^n)_{k\in\mathbb{Z}}$ has an exponential form provided that the prescribed moments U_i^n are strictly realizable (*i.e.* U_i^n is the moment vector of a strictly positive discrete function). In this case, the discrete equilibrium is $\mathcal{E}_{i,k}^n = \exp(\alpha_i^n \cdot m_k)$, where $\alpha_i^n \in \mathbb{R}^3$ is the solution of the discrete moment problem (see Appendix C for more details):

$$\sum_{k\in\mathbb{Z}} m_k \exp(\alpha_i^n \cdot m_k)\Delta v = U_i^n. \tag{3.3}$$

We note that (3.1) can be viewed as a first order finite volume method for the BGK equation (1.1), (1.2).

Now, in order to decompose the velocity domain, we have to define a discretized version of the ball B_1. In the remainder of this paper, we shall choose $\underline{u}$ and $\underline{T}$ as the global mean velocity $u(t,x)$ and temperature $T(t,x)$ respectively. They are approximated at point x_i and at time t^n by:

$$\underline{u}_i^n = \frac{P_i^n}{n_i^n}, \tag{3.4}$$

$$\underline{T}_i^n = \frac{2W_i^n n_i^n - (P_i^n)^2}{(n_i^n)^2}, \tag{3.5}$$

where n_i^n, P_i^n and W_i^n are the mass, momentum and energy at x_i and t^n, and are such that:

$$U_i^n = \begin{pmatrix} n_i^n \\ P_i^n \\ 2W_i^n \end{pmatrix} = \sum_{k\in\mathbb{Z}} f_{i,k}^n m_k \Delta v.$$

Then, at position x_i and time t^n, $(B_1)_i^n$ can be approximated by the following discrete set:

$$\mathcal{K}_i^n = \{k \in \mathbb{Z} \ \text{ s.t. } \ v_k = k\Delta v \ \text{ satisfies } \ |v_k - \underline{u}_i^n| \leq \mathcal{R}\sqrt{\underline{T}_i^n}\}, \tag{3.6}$$

where $\mathcal{R}$ is an arbitrary parameter.

We introduce the moments of $(f_{i,k}^n)_{k\in\mathbb{Z}}$ on the set $\mathcal{K}_i^n$ according to:

$$U_{1,i}^n = \sum_{k\in\mathcal{K}_i^n} m_k f_{i,k}^n \Delta v,$$

and the restriction of $(f_{i,k}^n)_{k\in\mathbb{Z}}$ on $\mathbb{Z}\setminus\mathcal{K}_i^n$:

$$f_{2,i,k}^n = \begin{cases} f_{i,k}^n & \text{if } k \in \mathbb{Z}\setminus\mathcal{K}_i^n \\ 0 & \text{otherwise.} \end{cases}$$

We are going to present an algorithm which, from the knowledge of $\mathcal{K}_i^n,\ U_{1,i}^n,\ f_{2,i,k}^n$ at time t^n, computes $\mathcal{K}_i^{n+1},\ U_{1,i}^{n+1},\ f_{2,i,k}^{n+1}$ at time t^{n+1}, based on the moments of (3.1).

First, the discrete fluxes on $\mathcal{K}_i^n$ of an arbitrary discrete distribution function $(g_k)_{k\in\mathbb{Z}}$ are denoted by:

$$\phi_{1,i,\pm}^n(g) = \sum_{k\in\mathcal{K}_i^n} v_k^{\pm} m_k g_k \Delta v, \tag{3.7}$$

and the moments of $(\mathcal{E}_{i,k}^n)_{k\in\mathbb{Z}}$ on $\mathcal{K}_i^n$ are written:

$$U_{(1),i}^n = \sum_{k\in\mathcal{K}_i^n} m_k \mathcal{E}_{i,k}^n \Delta v.$$

To close our discrete moment systems, we shall approximate $f_{i,k}^n$ on $\mathcal{K}_i^n$ by the solution $(\mathcal{M}_{1,i,k}^n)_{k\in\mathcal{K}_i^n}$ of the following minimization problem, with the prescribed moments $U_{1,i}^n$:

$$\text{Min}\left\{ \sum_{k\in\mathcal{K}_i^n} g_k \log(g_k)\Delta v,\ g_k \geq 0 \text{ s.t. } \sum_{k\in\mathcal{K}_i^n} m_k g_k \Delta v = U_{1,i}^n \right\}. \tag{3.8}$$

Note that (3.8) differs from (3.2) in that the summations are carried over the set $\mathcal{K}_i^n$ instead of $\mathbb{Z}$. This problem is solved in the same way as (3.2). Indeed, if the prescribed moments $U_{1,i}^n$ are strictly realizable, $\mathcal{M}_{1,i,k}^n$ has the following exponential form $\mathcal{M}_{1,i,k}^n = \exp(\lambda_{1,i}^n \cdot m_k)$, where $\lambda_{1,i}^n \in \mathbb{R}^3$ is the solution of the discrete moment problem:

$$\sum_{k\in\mathcal{K}_i^n} m_k \exp(\lambda_{1,i}^n \cdot m_k)\Delta v = U_{1,i}^n. \tag{3.9}$$

Now, we first take the moments of (3.1) on $\mathcal{K}_i^n$ and close the resulting equations by the discrete entropy minimization problem (3.8). In a next step, we shall "move" the set $\mathcal{K}_i^n$ into a new one, $\mathcal{K}_i^{n+1}$. First, let us introduce the moments $\tilde{U}_{1,i}^{n+1}$ of $f_{i,k}^{n+1}$ on the ball $\mathcal{K}_i^n$:

$$\tilde{U}_{1,i}^{n+1} = \sum_{k\in\mathcal{K}_i^n} m_k f_{i,k}^{n+1} \Delta v,$$

as well as the restriction of $f_{i,k}^{n+1}$ onto the complement $\mathbb{Z}\setminus\mathcal{K}_i^n$:

$$\tilde{f}_{2,i,k}^{n+1} = \begin{cases} f_{i,k}^{n+1} & \text{if } k \notin \mathcal{K}_i^n \\ 0 & \text{otherwise.} \end{cases}$$

If we take the discrete moments of (3.1) on $\mathcal{K}_i^n$, and close the resulting moment equations by the solution $f_{i,k}^n \simeq \mathcal{M}_{1,i,k}^n,\ \forall k \in \mathcal{K}_i^n$ of the discrete entropy minimization problem (3.8) on the one hand, and take the restriction of (3.1) on $\mathbb{Z}\setminus\mathcal{K}_i^n$ on the other hand, we obtain:

$$\begin{aligned} \tilde{U}_{1,i}^{n+1} = U_{1,i}^n &- \frac{\Delta t}{\Delta x}\left[\phi_{1,i,+}^n(\mathcal{M}_{1,i}^n) - \phi_{1,i,+}^n(\mathcal{M}_{1,i-1}^n + f_{2,i-1}^n)\right] \\ &- \frac{\Delta t}{\Delta x}\left[\phi_{1,i,-}^n(\mathcal{M}_{1,i+1}^n + f_{2,i+1}^n) - \phi_{1,i,-}^n(\mathcal{M}_{1,i}^n)\right] + \frac{\Delta t}{\tau}\left[U_{(1),i}^n - U_{1,i}^n\right], \end{aligned} \tag{3.10}$$

$$\tilde{f}^{n+1}_{2,i,k} = f^n_{2,i,k} - v_k^+ \frac{\Delta t}{\Delta x}\left[f^n_{2,i,k} - \left(\mathcal{M}^n_{1,i-1,k} + f^n_{2,i-1,k}\right)\right]$$

$$-v_k^- \frac{\Delta t}{\Delta x}\left[\left(\mathcal{M}^n_{1,i+1,k} + f^n_{2,i+1,k}\right) - f^n_{2,i,k}\right] + \frac{\Delta t}{\tau}\left[\mathcal{E}^n_{i,k} - f^n_{2,i,k}\right], \tag{3.11}$$

Let us remark that $\tilde{U}^{n+1}_{1,i}$ and $\tilde{f}^{n+1}_{2,i,k}$ are intermediate variables that only take account the space variation of $\mathcal{K}^n_i$ through the fluxes.

The next step of the algorithm is to consider the time variation of $\mathcal{K}^n_i$. To that purpose, we construct $(\tilde{\mathcal{M}}^{n+1}_{1,i,k})_{k\in\mathcal{K}^n_i}$ the discrete distribution solution to (3.8) with the prescribed moments $\tilde{U}^{n+1}_{1,i}$. Then we define an approximation of $f^{n+1}_{i,k}$, for all $k \in \mathbb{Z}$, solution to (3.1) by $\tilde{f}^{n+1}_{i,k}$ such that:

$$\tilde{f}^{n+1}_{i,k} = \begin{cases} \tilde{\mathcal{M}}^{n+1}_{1,i,k} & \text{if } k \in \mathcal{K}^n_i \\ \tilde{f}^{n+1}_{2,i,k} & \text{otherwise.} \end{cases} \tag{3.12}$$

Hence, the discrete moments of $\tilde{f}^{n+1}_{i,k}$ are an approximation of U^{n+1}_i. At this level, $\underline{u}^{n+1}_i, \underline{T}^{n+1}_i$ and $\mathcal{K}^{n+1}_i$ can then be defined through (3.4), (3.5) (with n replaced by $n+1$). The unknowns at the next time step are finally:

$$U^{n+1}_{1,i} = \sum_{k\in\mathcal{K}^{n+1}_i} m_k \tilde{f}^{n+1}_{i,k} \Delta v, \tag{3.13}$$

$$f^{n+1}_{2,i,k} = \tilde{f}^{n+1}_{i,k}|_{\mathbb{Z}\setminus\mathcal{K}^{n+1}_i}. \tag{3.14}$$

The following proposition presents some properties of the above scheme:

Proposition 3.1 *Equations (3.10)-(3.14) give a numerical scheme that preserves the total mass, momentum and energy. Moreover, let $(f^0_{i,k})_{i,k\in\mathbb{Z}}$ be a strictly positive initial condition:*

$$f^0_{i,k} > 0, \ \ \forall k \in \mathbb{Z}, \ \forall i \in \mathbb{Z}.$$

Let us denote by $\mathcal{K}$ a bounded discrete velocity domain which is an approximation of $\mathbb{Z}$. If the following condition on the time step is fulfilled:

$$\Delta t \left(\frac{1}{\tau} + \max_{k\in\mathcal{K}}\left(\frac{|v_k|}{\Delta x}\right)\right) < 1, \tag{3.15}$$

then the kinetic sequence $(f^n_{2,i,k})_{n\geq 0}$ defined by the above scheme, satisfies:

$$f^n_{2,i,k} > 0, \quad \text{for all } n \geq 0, \ i \in \mathbb{Z}, \ k \in \mathcal{K}\setminus\mathcal{K}^n_i. \tag{3.16}$$

Proof. We first prove the conservation property of the scheme. For this purpose, we introduce the discrete moments of $(f^n_{2,i,k})_k$:

$$U^n_{2,i} = \sum_{k\in\mathbb{Z}\setminus\mathcal{K}^n_i} m_k f^n_{2,i,k} \Delta v.$$

Let us multiply (3.11) by $m_k = (1, v_k, v_k^2)^T$ and sum over $k \in \mathbb{Z}\setminus\mathcal{K}^n_i$:

$$\sum_{k\in\mathbb{Z}\setminus\mathcal{K}^n_i} m_k \tilde{f}^{n+1}_{2,i,k}\Delta v = U^n_{2,i} - \frac{\Delta t}{\Delta x}\left[\sum_{k\in\mathbb{Z}\setminus\mathcal{K}^n_i} {v_k}^+ m_k \left(f^n_{2,i,k} - \left(f^n_{2,i-1,k} + \mathcal{M}^n_{1,i-1,k}\right)\right)\Delta v\right]$$

$$-\frac{\Delta t}{\Delta x}\left[\sum_{k\in\mathbb{Z}\setminus\mathcal{K}_i^n} {v_k}^- m_k\left((\mathcal{M}^n_{1,i+1,k}+f^n_{2,i+1,k})-f^n_{2,i,k}\right)\Delta v\right]$$

$$+\frac{\Delta t}{\tau}\left[\sum_{k\in\mathbb{Z}\setminus\mathcal{K}_i^n}(m_k\mathcal{E}^n_{i,k})\Delta v - U^n_{2,i}\right]. \tag{3.17}$$

If we add (3.17) with (3.10), and sum up over $i\in\mathbb{Z}$, the discrete fluxes vanish. As well, the discrete collision operator vanishes. Then, if we note:

$$\tilde{U}^{n+1}_{2,i}=\sum_{k\in\mathbb{Z}\setminus\mathcal{K}_i^n} m_k\tilde{f}^{n+1}_{2,i,k}\Delta v,$$

we obtain:

$$\sum_{i\in\mathbb{Z}}(\tilde{U}^{n+1}_{1,i}+\tilde{U}^{n+1}_{2,i})=\sum_{i\in\mathbb{Z}}(U^n_{1,i}+U^n_{2,i}).$$

The second step of the algorithm (3.13), (3.14) preserves the macroscopic quantities, so that we finally obtain:

$$\sum_{i\in\mathbb{Z}}U^{n+1}_i=\sum_{i\in\mathbb{Z}}U^n_i=C,$$

where C is a constant, only depending on the initial discrete mass, momentum and energy.

In order to show the positivity of the sequence $(f^n_{2,i,k})_{n\geq 0}$, let us write (3.11) as follows:

$$\tilde{f}^{n+1}_{2,i,k}=\left(1-\frac{\Delta t}{\tau}-|v_k|\frac{\Delta t}{\Delta x}\right)f^n_{2,i,k}+v_k^+\frac{\Delta t}{\Delta x}\mathcal{M}^n_{1,i-1,k}+v_k^+\frac{\Delta t}{\Delta x}f^n_{2,i-1,k}$$

$$-v_k^-\frac{\Delta t}{\Delta x}\mathcal{M}^n_{1,i+1,k}-v_k^-\frac{\Delta t}{\Delta x}f^n_{2,i+1,k}+\frac{\Delta t}{\tau}\mathcal{E}^n_{i,k},\ \text{for all } k\in\mathcal{K}\setminus\mathcal{K}_i^n,$$

with the notations: $v_k^\pm=\dfrac{v_k\pm|v_k|}{2}$, and $\mathcal{K}$ is a bounded discrete velocity domain. The strict positivity of $\tilde{f}^{n+1}_{2,i,k}$ is ensured if:

$$1-\frac{\Delta t}{\tau}-|v_k|\frac{\Delta t}{\Delta x}\geq 0,\ \ \forall k\in\mathcal{K},\ \forall i\in\mathbb{Z},$$

holds. Then, if we suppose the existence of $\tilde{\mathcal{M}}^{n+1}_{1,i,k},\ \forall k\in\mathcal{K}_i^n$, which is positive because it is a maxwellian, relations (3.13) and (3.14) ensure the positivity of $f^{n+1}_{2,i,k}$. □

Remark 3.2 *The property (3.16) of the above numerical scheme allows us to show that $\mathcal{E}^{n+1}_{i,k}$, and $\mathcal{M}^{n+1}_{1,i,k}$, have an exponential form with respect to k. Indeed, the strict positivity of $(\tilde{f}^{n+1}_{2,i,k})$ (under the condition on the time step (3.15) of proposition 3.1 ensures that U^{n+1}_i is the moment vector of a strictly positive discrete function (see (3.13)). According to [22], this implies that U^{n+1}_i is also a moment vector of a discrete maxwellian function $\mathcal{E}^{n+1}_{i,k}$, which uniquely solves the discrete entropy minimization problem (3.2). The same is true for the moments $U^{n+1}_{1,i}$.*

The resolution of the discrete entropy minimization problems (3.2) and (3.8) are classical ([22], [24]). For the sake of completeness, this step is detailed in Appendix C.

4 Numerical results:

In this section, we present numerical tests to illustrate the capabilities of the method. We validate our method on one-dimensional flows (shock tube problems). We also investigate the influence of the numerical parameters. Note that in this section, we go back to an equation using physical variables. In particular, τ is the relaxation time, t, x, v are respectively the time, space and velocity variables.

Numerically, the boundary conditions are treated by a classical ghost cell technique (see [31]). A Dirichlet or a reflecting condition is imposed in the ghost cell according to the test case.

Computations by means of the BGK model and the hybrid model take about the same amount of CPU time (slightly more for the hybrid model). However, at this stage, we did not try to optimize the numerical efficiency but wanted first to test the hybrid methodology in the most straightforward way. Indeed, the numerical fluxes (3.7) for the Euler equations are calculated by discrete integration of the maxwellian on phase space. Therefore, the complexity of the method is the same as for the resolution of the BGK model. Some pre-storage of these numerical fluxes will reduce the CPU time. Also, shifting from a finite volume method to a particle method for the discretization of the kinetic part should also greatly improve the efficiency of the method.

4.1 Shock tube problem: basic test problem:

We study a one-dimensional stationary shock wave (see [4], [22]). The flow is initialized with two maxwellian states related by the discrete Rankine-Hugoniot relations. Let us detail these discrete Rankine-Hugoniot relations:

For a given left state U_L, we must find a right state U_R such that there exists a stationary solution of the discrete BGK model (3.1), *i.e.*:

$$v_k \frac{\partial f_k}{\partial x} = \frac{1}{\tau}(\mathcal{E}_k - f_k), \ \ \forall k \in \mathbb{Z}, \tag{4.18}$$

with the boundary conditions:

$$f_k(-\infty) = \mathcal{E}_{k,L}, \quad \text{and} \quad f_k(+\infty) = \mathcal{E}_{k,R},$$

where $\sum_{k\in\mathbb{Z}} m_k \mathcal{E}_{k,L} \Delta v = U_L$ and $\sum_{k\in\mathbb{Z}} m_k \mathcal{E}_{k,R} \Delta v = U_R$. Multiplying (4.18) by m_k and summing on $k \in \mathbb{Z}$, we see that U_L and U_R must necessarily satisfy the following discrete Rankine-Hugoniot relations:

$$\sum_{k\in\mathbb{Z}} v_k m_k \mathcal{E}_{k,L} \Delta v = \sum_{k\in\mathbb{Z}} v_k m_k \mathcal{E}_{k,R} \Delta v.$$

To solve this problem, we use a Newton iterative algorithm in order to compute the downstream values of n, u, T as functions of the upstream ones.

We have used the following values for the mass density $n_L = 6.63 \times 10^{-6}\ kg.m^{-3}$, the mean velocity $u_L = 2551\ m.s^{-1}$, and temperature $T_L = 293\ K$, of the upstream flow. The gas considered is argon (the molecular mass m_A equals $66.3 \times 10^{-27} kg$). These values yield a shock Mach number equal to 6. The computational domain is $[0, L]$, $L = 1\ m$ whereas the

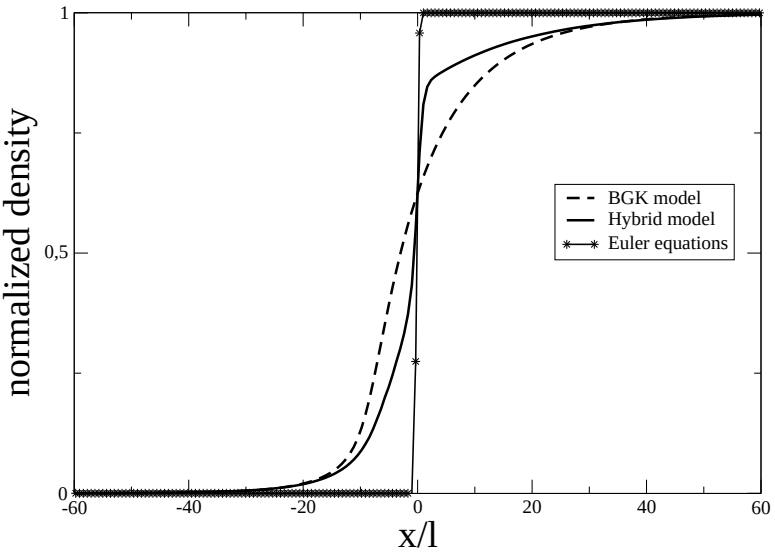

Figure 1: Stationary shock: Normalized mass density as a function of x/l, $x \in [0, L]$. The Mach number of the flow is 6. Comparison between the BGK model (dashed line), the hybrid model (continuous) and the Euler equations (stars).

velocity domain takes into account the discrete velocities between $v_{min} = (-5600)\ m.s^{-1}$ and $v_{max} = 8200\ m.s^{-1}$. A one-dimensional grid of 200 cells in space and 200 cells in velocity is used. The constant parameter $\mathcal{R}$ is taken equal to 2 and τ equals $3 \times 10^{-5}\ s$.

In Figs. 1, 2, and 3, we present the normalized profiles $(q - q_L)/(q_R - q_L)$ for $q = n$ (the mass density), $q = u$ (the mean velocity) and $q = T$ (the temperature) as functions of the normalized space variable x/l (where l is the mean free path of the upstream flow ($l = \tau\sqrt{RT_L}$, where R is the gas constant)). These figures display the results obtained by the hybrid model, by the full BGK equation (discretized by (3.1)) and by the Euler equations (discretized following [13]). The velocity set (given by $[v_{min}, v_{max}]$) ensures that the left and right maxwellians are correctly represented. The stationary shock wave of the Euler equations is situated at $x = 0.5\ m$. On Figs. 1, 2, and 3, we can see that the hybrid model is closer to the BGK model than to the Euler equations, but the shock wave of the hybrid model is stiffer than that of the BGK model. The hybrid model has an intermediate behaviour between the Euler equations and the BGK model, as could be expected.

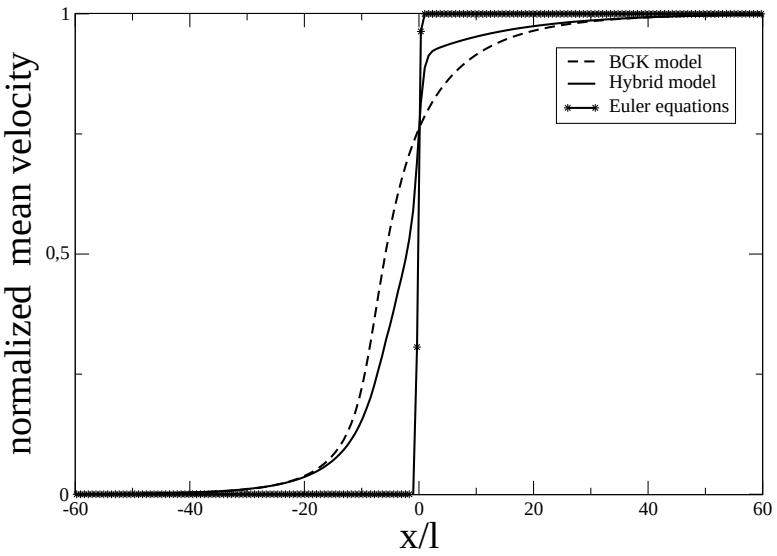

Figure 2: Stationary shock: Normalized mean velocity as a function of $x/l,\ x \in [0, L]$. The Mach number of the flow is 6. Comparison between the BGK model (dashed line), the hybrid model (continuous) and the Euler equations (stars).

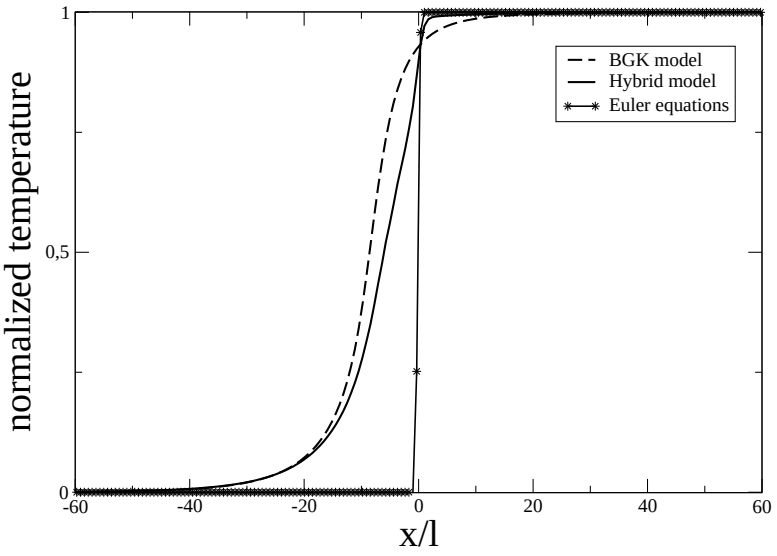

Figure 3: Stationary shock: Normalized temperature as a function of $x/l,\ x \in [0, L]$. The Mach number of the flow is 6. Comparison between the BGK model (dashed line), the hybrid model (continuous) and the Euler equations (stars).

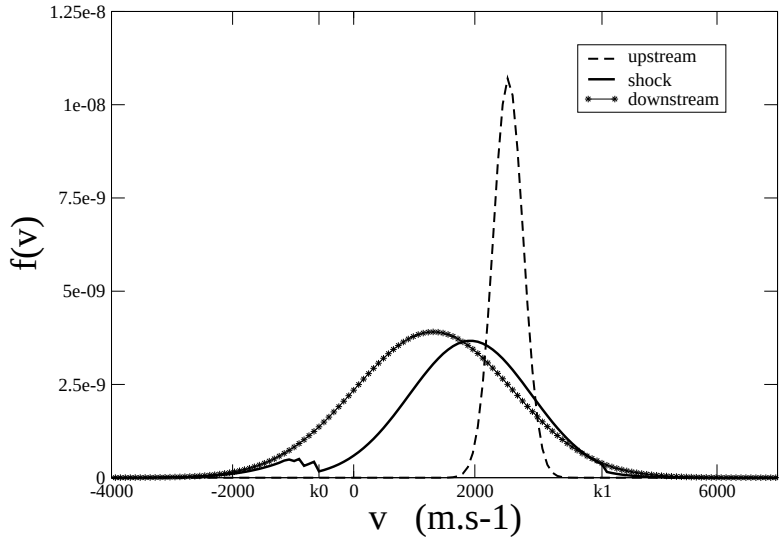

Figure 4: Stationary shock: Distribution functions as functions of the velocity $v \in [v_{min}, v_{max}]$. The Mach number of the flow is 6. Distribution functions upstream the shock ($x = 0.1\ m$) (dashed line), inside the shock ($x = 0.5\ m$) (continuous line) and downstream the shock ($x = 0.9\ m$) (stars) are presented. $B_1 = [k_0, k_1]$ is the fluid zone at $x = 0.5\ m$.

The distribution functions computed by the hybrid model at locations upstream ($x = 0.1\ m$), within ($x = 0.5\ m$) and downstream ($x = 0.9\ m$) the shock, are plotted on Fig. 4 as functions of the velocity $v \in [v_{min}, v_{max}]$. When the flow is at equilibrium (upstream and downstream the shock), the distribution functions are very well approximated by the hybrid model. Inside the shock, the hybrid model computes an intermediate maxwellian between the upstream and downstream maxwellians, with a jump at the boundary of the ball $v = k_0$ (where k_0 is s.t. $B_1 = [k_0, k_1]$). The departure from equilibrium of the distribution function inside the shock is not accurately enough described by the hybrid model. On Fig. 5, we can see the distribution functions of the hybrid model and of the full BGK model within the shock, as functions of the velocity; we can see a jump at $v = k_0$ for the hybrid model; this is a discontinuity between the kinetic unknown f_2 and the maxwellian $\mathcal{M}_1$.

On Fig. 6, we present the distribution functions of the hybrid model and of the full BGK model, as functions of the velocity, at $x = 0.54\ m$. The BGK distribution function has two humps of comparable size whereas a maxwellian (with one hump only) takes place for the hybrid model. This figure shows the limit of our approach. Indeed, the hybrid model makes some errors in describing the distribution function inside the shock.

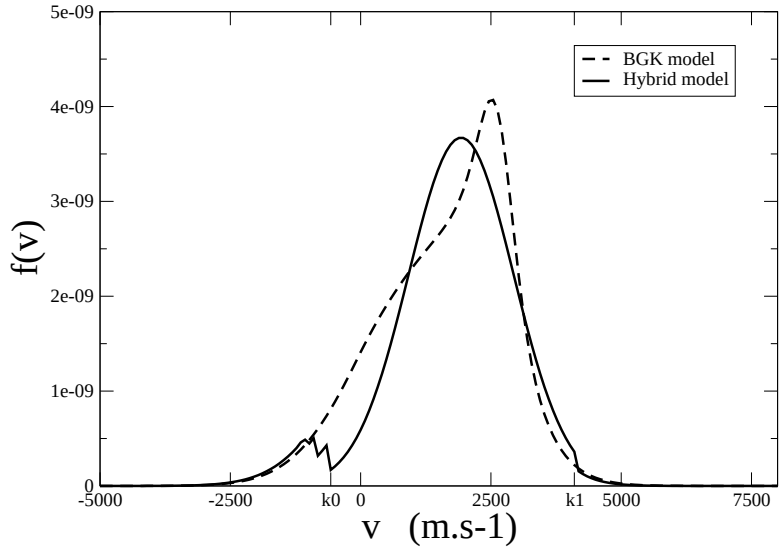

Figure 5: Stationary shock: Distribution functions as functions of the velocity $v \in [v_{min}, v_{max}]$. The Mach number of the flow is 6. Distribution functions within the shock ($x = 0.5\ m$). Comparison between the full BGK model (dashed line) and the hybrid model (continuous). $B_1 = [k_0, k_1]$ is the fluid zone at $x = 0.5\ m$.

4.2 Shock tube problem: Influence of the numerical parameters:

In this subsection, we present the influence of the numerical parameters on both the macroscopic and microscopic quantities. First, we study the influence of the velocity discretization, while the other parameters are kept fixed to the values $\Delta x = \frac{1}{200}, \mathcal{R} = 2, \tau = 3 \times 10^{-5}\ s.$ and $\Delta t = 6 \times 10^{-7}$; Fig. 7 represents the normalized mass density as a function of the normalized space variable $x/l,\ x \in [0, L],\ (L = 1\ m)$, where l is the upstream mean free path, obtained by the hybrid model with different velocity discretizations. We can see that the increase of the number of discrete velocities does not improve the results significantly. Nevertheless, a minimal number of discrete points in velocity space is needed. Indeed, we need a sufficient number of discrete velocities in the discrete ball in order to solve the discrete moment problem (3.8) (see Appendix C).

We also study the influence of the space discretization. Fig. 8 represents the normalized mass density as a function of the normalized space variable $x/l,\ x \in [0, L]$, obtained with different values of Δx (and with $\mathcal{R} = 2,\ \tau = 3 \times 10^{-5}\ s.$, 200 discrete velocities and $\Delta t = 6 \times 10^{-7}$). We can see that the shock becomes stiffer as Δx is decreased, up to $\frac{\Delta x}{L} = \frac{1}{400}$. The same behaviour is observed for the mean velocity and the temperature. The value $\Delta x = \frac{1}{200}$ seems to be a good compromise between accuracy and computer time.

The variation of Δt does not improve the results (with $\mathcal{R} = 2$, $\tau = 3 \times 10^{-5}\ s.$, 200 discrete velocities and $\Delta x = \frac{1}{200}$). Indeed, the condition (3.15) imposes a small time step which already gives some quite good results ($\Delta t = 6 \times 10^{-7}$). In Fig. 9, we can see the normalized mass density as a function of the normalized space variable $x/l,\ x \in [0, L]$, obtained by the hybrid model with different values of Δt.

Once the numerical parameters are chosen properly, we investigate the influence of the

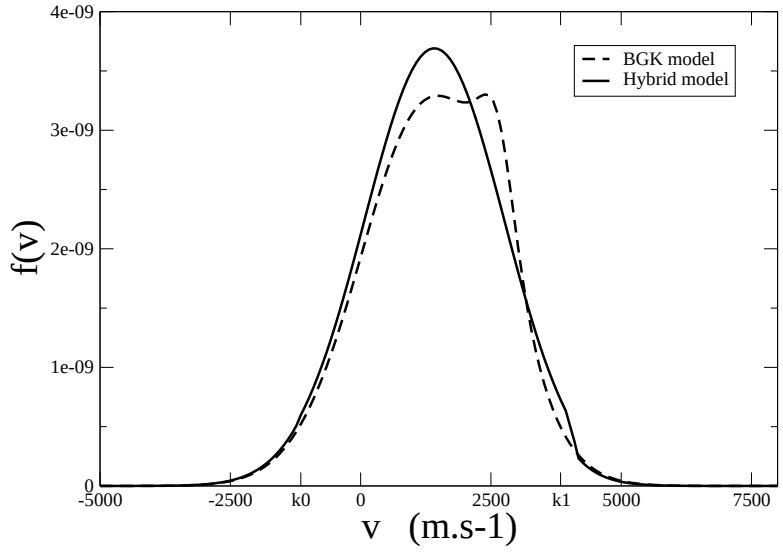

Figure 6: Stationary shock wave: Distribution functions as functions of the velocity $v \in [v_{min}, v_{max}]$. The Mach number of the flow is 6. The distribution functions at $x = 0.54\ m$ are represented. Comparison between the full BGK model (dashed line) and the hybrid model (continuous).

parameter $\mathcal{R}$ on both the macroscopic and microscopic quantities. The parameter $\mathcal{R}$ is a kind of cutover between Maxwellian and kinetic solvers. By varying $\mathcal{R}$, we cross between the pure fluid description (large $\mathcal{R}$) to the full kinetic one (small $\mathcal{R}$). The other parameters are taken as follows: $\tau = 3 \times 10^{-5}\ s.$, $\Delta t = 6 \times 10^{-7}$, 200 discrete velocities and $\Delta x = \frac{1}{200}$. For instance, on Fig. 10, we plot the distribution functions within the shock ($x = 0.5\ m$) as functions of the velocity $v \in [v_{min}, v_{max}]$ for the hybrid model with various values of $\mathcal{R}$, and for the full BGK model. In the same way, on Fig. 11, the normalized mass density profile is plotted as a function of the normalized space variable x/l for the hybrid model (for different value of $\mathcal{R}$) and for the full BGK model in comparison. When $\mathcal{R}$ is small ($\mathcal{R} = 0.5$ or $\mathcal{R} = 1$), both microscopic and macroscopic quantities are in good agreement with results given by the BGK model. On the contrary, as $\mathcal{R}$ is growing, the macroscopic profiles (Fig. 11 and the same is true for the mean velocity and the temperature) become less smooth and tend towards the results given by the Euler equations. In the same way, the distribution function inside the shock given by the hybrid model is very close to that given by the BGK model for small values of $\mathcal{R}$ ($\mathcal{R} = 0.5$ or $\mathcal{R} = 1$ for example). When $\mathcal{R}$ is greater ($\mathcal{R} = 3$), the distribution function (Fig. 10) becomes a maxwellian (like that given by the Euler equations). In this case, the hybrid model does not describe accurately the results of the BGK model. As pointed out in the introduction, we focused on the validation of the hybrid model without any consideration about the numerical cost. In particular, the numerical cost does not depend on $\mathcal{R}$. The a priori choice of $\mathcal{R} = 2$ seems to be a good compromise. Note that the parameter $\mathcal{R}$ may depend on the space variable x. This allows to choose a suitable $\mathcal{R}$, which is small at locations where the flow is known to be far from equilibrium and large when the flow is close to the equilibrium. For example, in the case of a stationary shock wave, a smaller $\mathcal{R}$ can be used within the shock while a larger $\mathcal{R}$ is sufficient to describe the flow far from the shock.

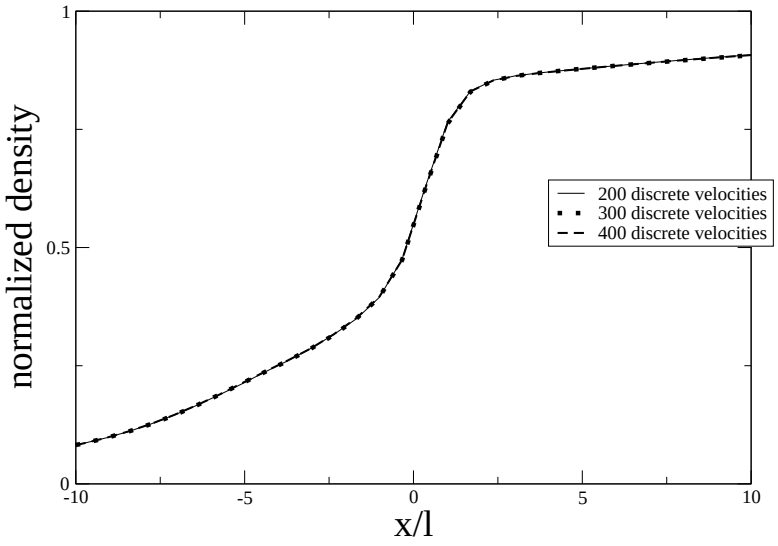

Figure 7: Stationary shock: Influence of the number of discrete velocities on the normalized mass density as a function of x/l, $x \in [0, L]$. The Mach number of the flow is 6. Results obtained with 100 (continuous line), 200 (dotted line) and 400 discrete velocities (dashed line) are presented.

Finally, on Fig. 12, we have plotted the inverse of the shock-wave thickness as a function of the upstream Mach number (see [4] and [22]). We define the shock-wave thickness, for instance for the mass density, by the length L_S s.t.:

$$L_S = \frac{n_R - n_L}{\left(\frac{dn}{dx}\right)_{max}},$$

where n_R and n_L are the downstream and upstream mass densities respectively. As mentionned above, when $\mathcal{R}$ is large ($\mathcal{R} = 3, 4$), the shock-wave thickness of the hybrid model is smaller than that of the BGK model. When $\mathcal{R} = 0.5$ or $\mathcal{R} = 1$, the thickness L_S of the hybrid model is comparable with that of the BGK model. Our results seem to be in good agreement with the experimental data, up to Mach 5 or Mach 6 (see [4] and [22]).

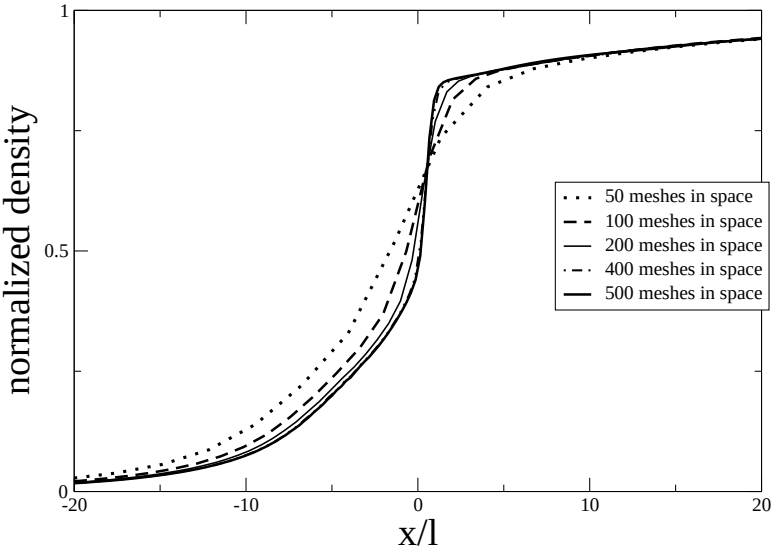

Figure 8: Stationary shock: Influence of the space discretization on the normalized mass density as a function of $x/l,\ x \in [0, L]$. The Mach number of the flow is 6. Results obtained with 50 (dotted line), 100 (dashed line), 200 (continuous), 400 (dashed and dotted line) and 500 mesh points (thick continuous line) are presented.

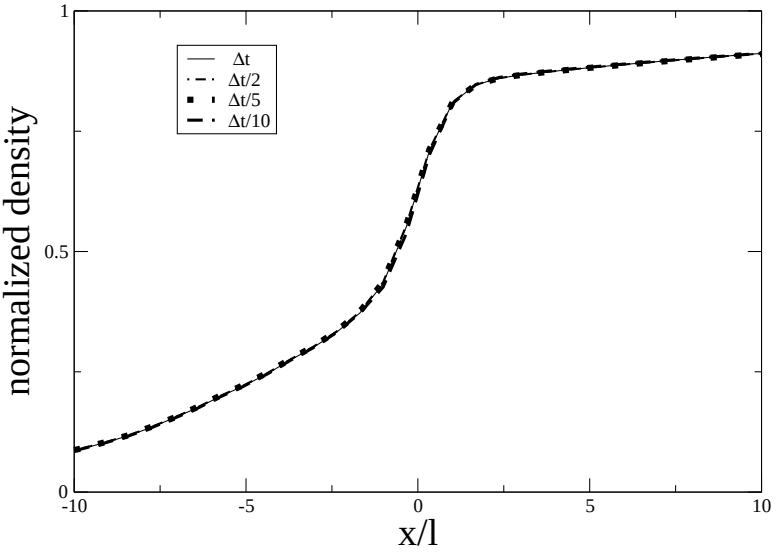

Figure 9: Stationary shock: Influence of the time step on the normalized mass density as a function of $x/l,\ x \in [0, L]$. The Mach number of the flow is 6. Results obtained with Δt (continuous), $\Delta t/2$ (dashed and dotted line), $\Delta t/5$ (dotted line) and $\Delta t/10$ (thick dashed line) are presented ($\Delta t = 6 \times 10^{-7}$).

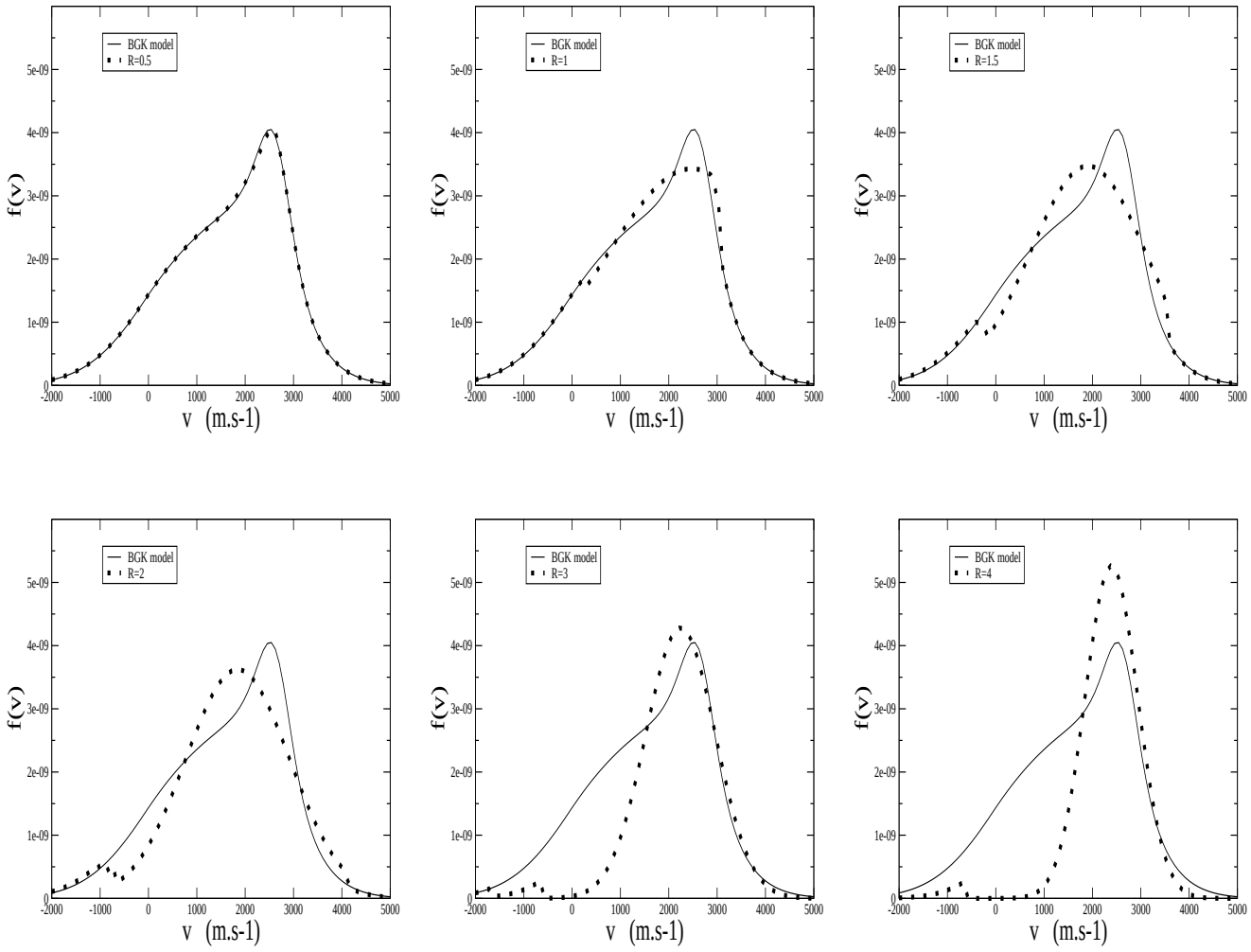

Figure 10: Stationary shock: Influence of the parameter $\mathcal{R}$ on the normalized mass density as a function of $x/l,\ x \in [0, L]$. The Mach number of the flow is 6.

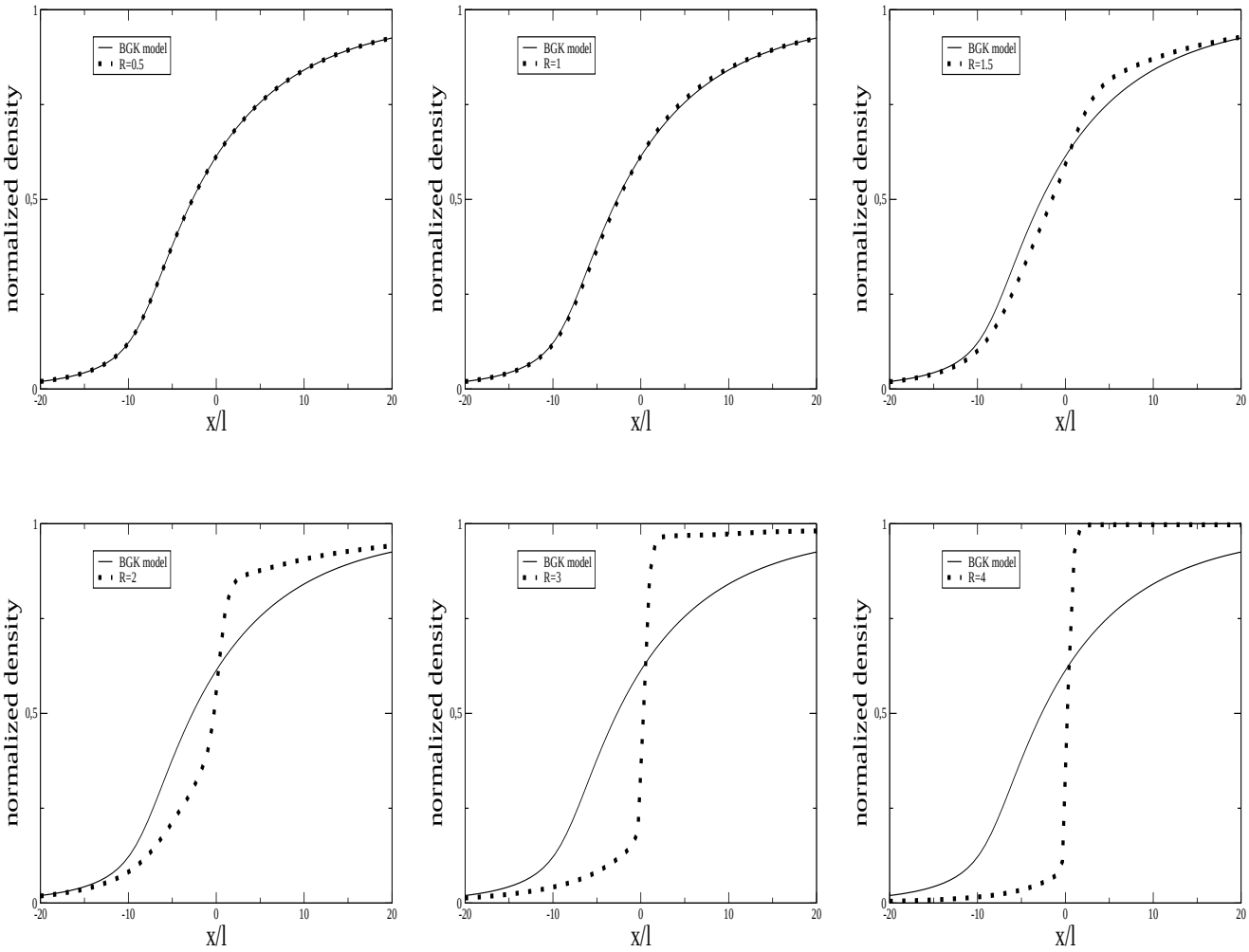

Figure 11: Stationary shock: Influence of the parameter $\mathcal{R}$ on the normalized mass density as a function of $x/l,\ x \in [0, L]$. The Mach number of the flow is 6.

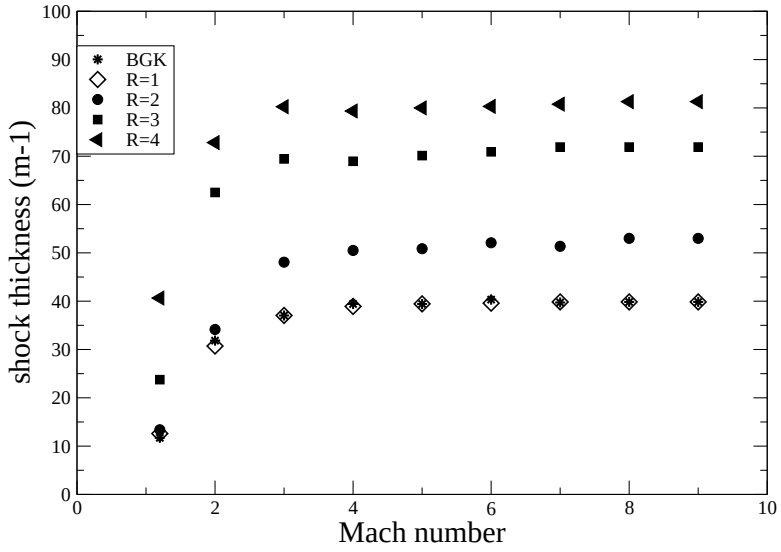

Figure 12: Shock-wave thickness as a function of the Mach number.

4.3 Sod shock tube problem:

In this section, we present an other numerical test, the Sod shock tube problem (see [30], [28]). We compare the hybrid model to the discrete BGK model (3.1) and to the exact solution of the Sod shock tube problem. The initial conditions are the following: the mass density $n_L = 1\ kg.m^{-3}$, the mean velocity $u_L = 0\ m.s^{-1}$ and the pressure $p_L = 10^5\ Pa$ for $x \in [0, L/2],\ L = 1\ m$, and the mass density $n_R = 0.125\ kg.m^{-3}$, the mean velocity $u_R = 0\ m.s^{-1}$ and the pressure $p_R = 10^4\ Pa$ for $x \in [L/2, L]$ The numerical parameters are: 200 cells in space ($\Delta x = 1/200$), 100 cells in velocity ($\Delta v = 15$) and $\Delta t = 2.5 \times 10^{-6}$. Moreover $\tau = 10^{-5}\ s.$ and $\mathcal{R} = 2$. The solution is observed at $0.52\ ms$.

Figs. 13, 14 and 15 respectively represent the mass density, mean velocity and pressure (circles) profiles as functions of the space variable x for the hybrid model. We have also plotted the numerical solution of the BGK model (continuous curves) and the exact solution of the Euler equations (discontinuous curves). We see that the rarefaction wave, the contact discontinuity and the shock wave are well described by the hybrid model. The hybrid numerical solution can be nearly superimposed on the BGK solution. On Fig. 14, we can see a bump at the contact discontinuity level. This bump seems to remain even when the time, space and velocity steps decrease (see [28]).

4.4 Unsteady shock problem:

We compare the results obtained by our hybrid model, with those obtained by the full BGK model and by the Euler equations, in the case of an unsteady shock wave (see [15], [7], and [4]).

The calculations are made in an unsteady fashion by using a classical procedure to produce a shock. At the beginning, the flow is uniform with a mass density $n = 10^{-6}\ kg.m^{-3}$, a mean velocity $u = -900\ m.s^{-1}$ and a temperature $T = 273\ K$. The gas considered is argon, as in the steady case (see section 4.1); at $x = 0\ m$, we put a specular wall and at $x = 2.5\ m$, an incoming

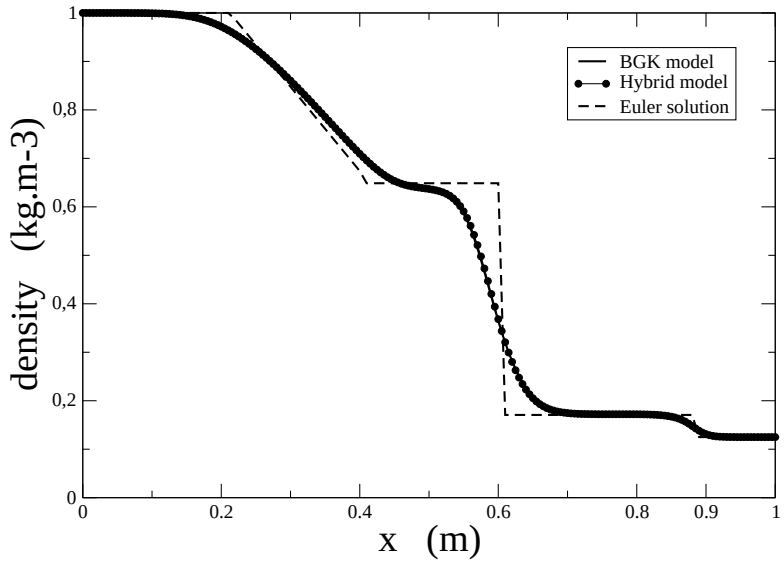

Figure 13: Sod shock tube problem: Mass density as a function of $x \in [0, L]$. Comparison between the BGK model (continuous), the hybrid model (circles) and the exact solution of the Euler equations (dashed line).

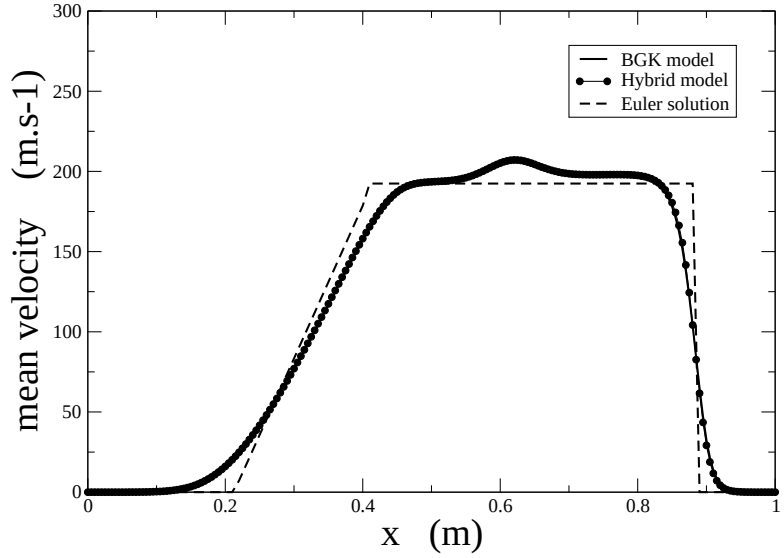

Figure 14: Sod shock tube problem: Mean velocity as a function of $x \in [0, L]$. Comparison between the BGK model (continuous), the hybrid model (circles) and the exact solution of the Euler equations (dashed line).

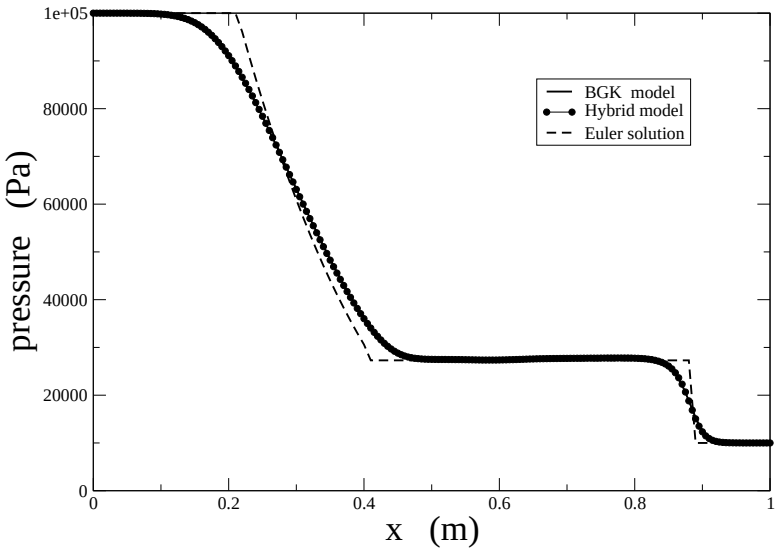

Figure 15: Sod shock tube problem: Pressure as a function of $x \in [0, L]$. Comparison between the BGK model (continuous), the hybrid model (circles) and the exact solution of the Euler equations (dashed line).

distribution equal to a maxwellian with parameters (n, u, T) is imposed in the ghost cell. We look at the solution when the shock arrives at a distance 1.6 m of the wall, which corresponds to $t = 1.64\ ms$.

The space domain $[0, 2.5]\ m$ is discretized using 500 mesh points, and we consider 140 discrete velocities in $[-4000, 4000]\ m.s^{-1}$. Moreover $\tau = 3 \times 10^{-5}\ s.$ and $\mathcal{R} = 2$. On Figs. 16, 17, 18, comparison between the three models are made on the macroscopic profiles (mass density, mean velocity and temperature). As in the steady case, the hybrid model has an intermediate behaviour between the BGK model and the Euler equations.

On Fig. 19, we study the influence of the parameter $\mathcal{R}$ on the mass density. When $\mathcal{R}$ is small ($\mathcal{R} = 1$), the results obtained thanks to the hybrid model are nearly superimposed on those given by the BGK model. On the contrary, as $\mathcal{R}$ is growing, our hybrid model gets closer to the Euler equations. The same conclusions hold for the mean velocity and the temperature.

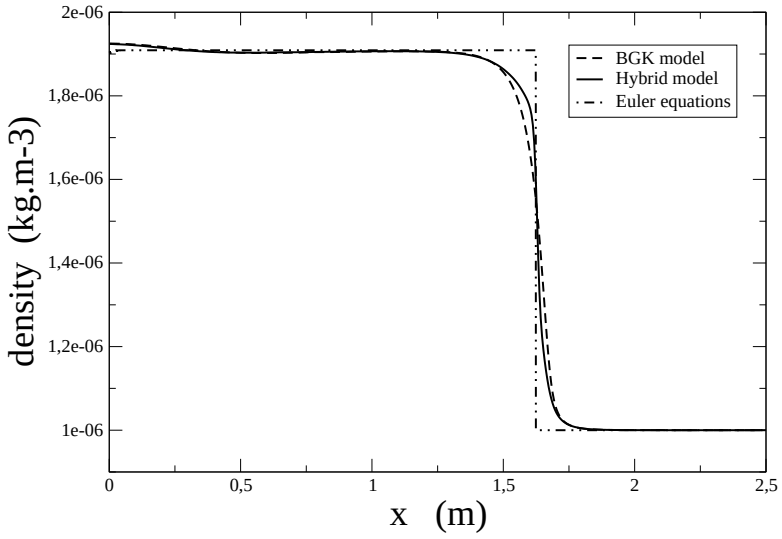

Figure 16: Unsteady shock: Mass density as a function of the space variable $x \in [0, 2.5]$ m. Comparison between the BGK model (dashed line), the hybrid model (continuous) and the Euler equations (dashed and dotted line).

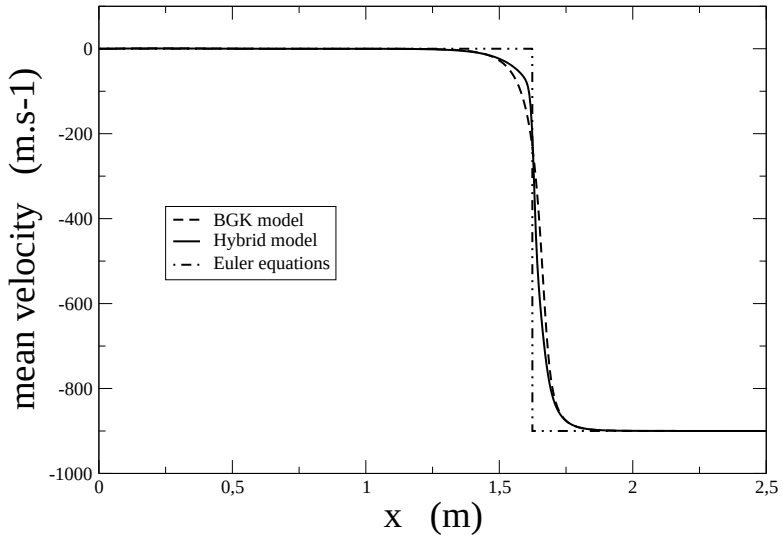

Figure 17: Unsteady shock: Mean velocity as a function of the space variable $x \in [0, 2.5]$ m. Comparison between the BGK model (dashed line), the hybrid model (continuous) and the Euler equations (dashed and dotted line).

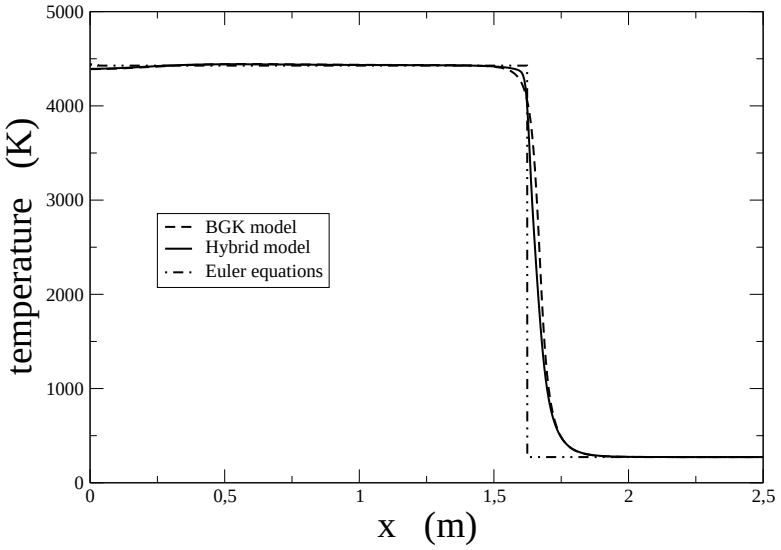

Figure 18: Unsteady shock: Temperature as a function of the space variable $x \in [0, 2.5]$ m. Comparison between the BGK model (dashed line), the hybrid model (continuous) and the Euler equations (dashed and dotted line).

5 Conclusion

First, we have presented a new hybrid model to describe systems of particles which are far from equilibrium. This model is based on a domain decomposition in velocity space and a fluid approximation of the solution of the kinetic equation for small velocities, based on a entropy minimization principle. The associated moment problems are rigourosly treated.

Second, we give a discrete version to this hybrid model. In particular, we obtain a numerical scheme preserving the total mass, momentum and energy of the system. Numerical results show that this method gives accurate results for the computation of transition regimes. In such regimes, the Euler or Navier-Stokes models are known to be insufficient to describe the flow. So far, our hybrid strategy is as costly as a direct resolution of the BGK model. Optimization procedure will be investigated in future work. However, the present work is a basis for the development of intermediate models between kinetic and fluid ones aiming at the description of transition regimes.

The approach will be further extended to more realistic collision operator. Moreover, the effect of an electrical field will be incorporated. These extensions will be the subject of future works.

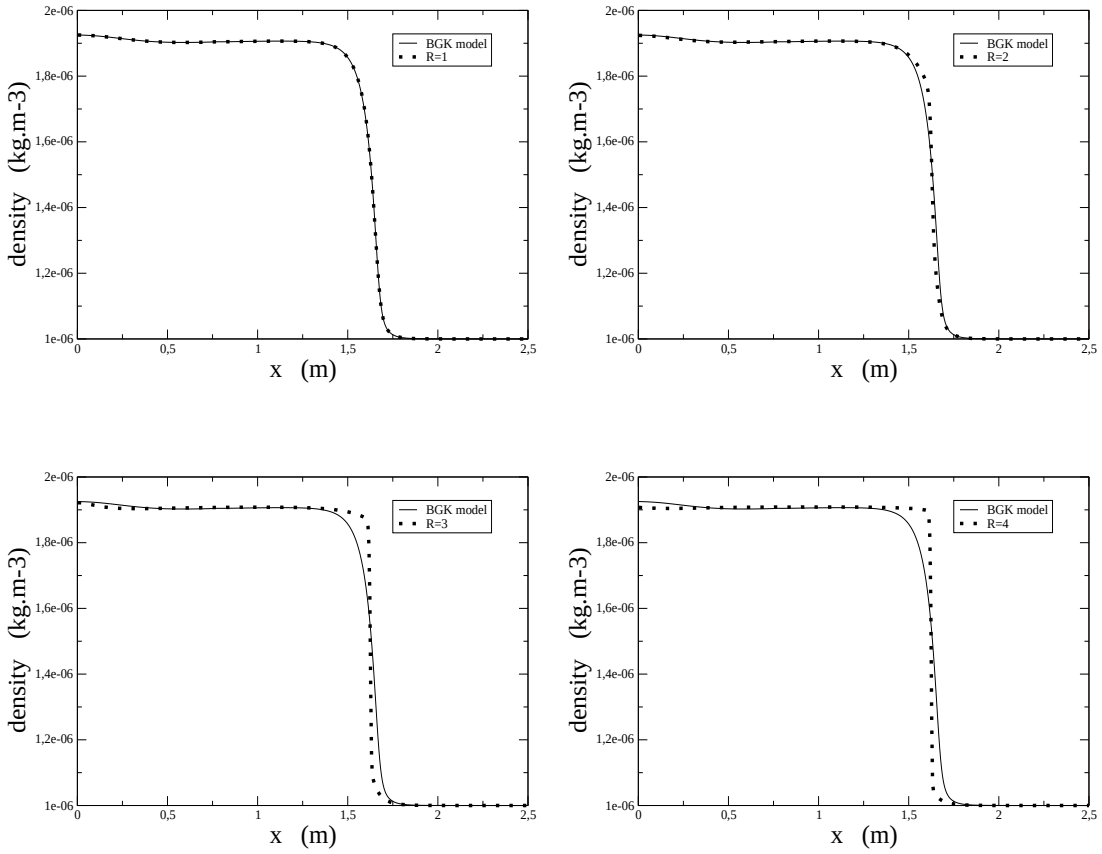

Figure 19: Unsteady shock: Influence of the parameter $\mathcal{R}$ on the mass density as a function of the space variable $x \in [0, 2.5]$ m.

5.1 Appendix A: Resolution of the entropy minimization problem:

This section is devoted to the resolution of the entropy minimization problem (2.2). We shall prove that (2.2) has a unique solution provided that the prescribed moments satisfy some constraints that will be precised later on. In order to make this statement precise, wee first need to specify what is known as the moment realizability problem: what necessary and sufficient conditions have to be satisfied by the prescribed moments n_1, P_1, W_1 so that the moment problem:

$$\left\{ \begin{array}{l} \text{Find a nonnegative function } \mathcal{M}_1 \text{ on } B_1 \text{ such that} \\ \displaystyle\int_{B_1} \mathcal{M}_1(v) \begin{pmatrix} 1 \\ v \\ |v|^2 \end{pmatrix} dv = \begin{pmatrix} n_1 \\ P_1 \\ 2W_1 \end{pmatrix} \end{array} \right. \tag{5.1}$$

admits at least one solution? When the moment realizability problem is solvable, the question is then: what are the necessary and sufficient conditions on n_1, P_1, W_1 so that the entropy minimization problem (2.2) admits a solution?

The proof is similar to that of [12] which uses results of [20]. To make the conditions such that (2.2) admits a solution explicit, we will use the following result borrowed from [20] (Theorem 7.1 and Theorem A.1):

Theorem 5.1 *[20] Let Ω be an open subset of $\mathbb{R}^d, d = 1, 2, 3$; consider $N+1$ independent moment functions $(a_i(x), i = 0..N)$ of the variable $x \in \Omega$ (where Ω is an open subset of $\mathbb{R}^d$), satisfying:*

$$a_N(x) \geq 0 \text{ and } \frac{|a_i(x)|}{1 + a_N(x)} \longrightarrow 0 \quad \text{as } |x| \to +\infty, \quad \text{for } i = 0..N-1.$$

Let D be the following functional domain:

$$D = \{f \geq 0, f \neq 0 \text{ and } \int_\Omega |(1 + a_N(x))f(x)|dx < +\infty\}.$$

For any $f \in D$, we consider the moment vector $\mu(f) = (\mu_0, \mu_1, ..., \mu_N)(f)$ defined by:

$$\mu(f) = \int_\Omega a(x)f(x)dx, \quad \text{with } a = (a_0, a_1, ..., a_N)^T.$$

The exponential functions are the functions of the form:

$$\exp_\lambda(x) = \exp(\lambda_0 a_0(x) + \lambda_1 a_1(x) + ... + \lambda_N a_N(x)), \tag{5.2}$$

with $\lambda = (\lambda_0, \lambda_1, ..., \lambda_N) \in \mathbb{R}^{N+1}$. We then define the following subset of $\mathbb{R}^{N+1}$:

$$\Lambda = \{\lambda \in \mathbb{R}^{N+1} \text{ s.t. } \exp_\lambda \in D\},$$

and denote $\partial\Lambda$ its boundary. Finally, we note:

$$E = \{\exp_\lambda \text{ s.t. } \lambda \in \Lambda\}.$$

(i)Then the following moment problem:

$$\text{For } \rho \in \mathbb{R}^{N+1},\ \text{find } f \in D \text{ s.t. } \mu(f) = \rho,$$

admits a solution if and only if, for all $\beta \in \mathbb{R}^{N+1} \setminus \{0\}$, *we have*

$$\beta \cdot a(x) \leq 0 \text{ a.e.} \Longrightarrow \beta \cdot \rho \leq 0.$$

(ii) Assume that $\Lambda \neq \emptyset$ *and* $\Lambda \cap \partial\Lambda = \emptyset$. *Then* $\mu(D) = \mu(E)$ *ie:*

$$\text{For all } \rho \in \mu(D),\ \text{there is an unique } \lambda \in \Lambda \text{ s.t. } \mu(\exp_\lambda) = \rho.$$

Moreover the entropy minimization problem:

$$Min\left\{\int_\Omega f \log f dx,\ \ f \geq 0 \text{ s.t. } \mu(f) = \rho\right\}$$

is uniquely solvable for all $\rho \in \mu(D)$.

Using this theorem, we will prove the proposition 2.3:

Proof of the proposition 2.3:

Thanks to (ii) of Theorem 5.1, we only have to show that the moment problem has a solution in the form of an exponential function. In fact, here we have $\Lambda = \mathbb{R}^{d+2}$ and $\Lambda \cap \partial\Lambda = \emptyset$. To show that the moment problem has a solution in the form of an exponential function, we use (i) of Theorem 5.1.

To get conditions (2.3), (2.4), we first rewrite the moment problem (5.1) as follows:

$$\text{find } f \ \text{ s.t. } \ \int_{B_1} f(v) \begin{pmatrix} 1 \\ \frac{v-\underline{u}}{\mathcal{R}\sqrt{\underline{T}}} \\ \frac{|v-\underline{u}|^2}{\mathcal{R}^2\underline{T}} \end{pmatrix} dv = \begin{pmatrix} n_1 \\ \frac{P_1 - \underline{u}n_1}{\mathcal{R}\sqrt{\underline{T}}} \\ \frac{1}{\mathcal{R}^2\underline{T}}(2W_1 - 2\underline{u}\cdot P_1 + |\underline{u}|^2 n_1) \end{pmatrix}.$$

The change of variables $w = \frac{v-\underline{u}}{\mathcal{R}\sqrt{\underline{T}}}$ leads to:

$$\int_{B(0,1)} f(\mathcal{R}\sqrt{\underline{T}}w + \underline{u}) \begin{pmatrix} 1 \\ w \\ |w|^2 \end{pmatrix} dw = (\mathcal{R}\sqrt{\underline{T}})^{-3} \begin{pmatrix} M_0 \\ M_1 \\ M_2 \end{pmatrix}, \tag{5.3}$$

with $B(0,1)$ the unit ball and

$$M_0 = n_1,$$
$$M_1 = \frac{P_1 - \underline{u}n_1}{\mathcal{R}\sqrt{\underline{T}}},$$
$$M_2 = \frac{2W_1 - 2\underline{u}\cdot P_1 + |\underline{u}|^2 n_1}{\mathcal{R}^2\underline{T}}.$$

We will prove that (5.3) has a solution. For that purpose, we use assertion (i) of Theorem 5.1 with $\Omega = B(0,1)$ and:

$$a_0(w) = 1,\ a_1(w) = w \quad (a_1 \in \mathbb{R}^d) \ \text{ and } \ a_2(w) = |w|^2.$$

Theorem 5.1 says that (5.3) has a solution if and only if, for all $(\beta_0, \beta_1, \beta_2)$ s.t. $\beta_0 + \beta_1 \cdot w + \beta_2 |w|^2 \leq 0,\ \forall w \in B(0,1)$, we have:

$$\beta_0 M_0 + \beta_1 \cdot M_1 + \beta_2 M_2 \leq 0.$$

Passing in polar coordinates in the first inequality, we obtain:

$$\beta_0 + \beta_1 \cdot w + \beta_2 |w|^2 = \beta_0 + |\beta_1||w| \cos\theta + \beta_2 |w|^2,\ \forall w \in B(0,1),\ \forall \theta \in [0, 2\pi]. \tag{5.4}$$

The second member of (5.4) is negative $\forall w \in B(0,1),\ \forall \theta \in [0, 2\pi]$ if and only if $\beta_0 + |\beta_1| X + \beta_2 X^2$ is negative $\forall X \in [0,1]$ (we set $X = |w|$).

We now characterize the set $\mathcal{C} = \Big\{(\beta_0, \beta_1, \beta_2)$ s.t. $\beta_0 + |\beta_1| X + \beta_2 X^2 \leq 0,\ \forall X \in [0,1]\Big\}$. Looking at the asymptotic behavior when X goes to zero and to 1, we get : $\beta_0 \leq 0$ and $\beta_0 + |\beta_1| + \beta_2 \leq 0$. For the function $F(X) = \beta_0 + |\beta_1| X + \beta_2 X^2$ to be negative for all $X \in [0,1]$, it is necessary and sufficient that its maximum remains negative. We then compute the maximum of the function F. If the critical point $\overline{X} = -\frac{|\beta_1|}{2\beta_2}$ belongs to $[0,1]$, $F(\overline{X}) \leq 0$ is equivalent to $F(X) \leq 0, \forall X \in [0,1]$ (because of the strict concavity of F ($\beta_2 < 0$)). On the other hand, if $\overline{X} \notin [0,1]$, $\max(F(0), F(1)) \leq 0$ is an equivalent condition to $F(X) \leq 0, \forall X \in [0,1]$. We find: $F(\overline{X}) = \beta_0 - \frac{|\beta_1|^2}{4\beta_2}$. Therefore,

$$\mathcal{C} = \Big\{(\beta_0, \beta_1, \beta_2) / \Big(-\frac{|\beta_1|}{2\beta_2} \in [0,1] \ \text{ and } \ \beta_0 - \frac{|\beta_1|^2}{4\beta_2} \leq 0 \Big)$$

$$\text{or } \Big(\beta_0 \leq 0,\ \beta_0 + |\beta_1| + \beta_2 \leq 0,\ \frac{-|\beta_1|}{2\beta_2} \notin [0,1]\Big)\Big\}.$$

Assertion (i) of Theorem 5.1 says that for all $\beta \in \mathcal{C}$, we have $\beta_0 M_0 + \beta_1 \cdot M_1 + \beta_2 M_2 \leq 0$, or equivalently $\beta_0 M_0 + |\beta_1||M_1| + \beta_2 M_2 \leq 0$.

If we first consider β s.t. $-\frac{|\beta_1|}{2\beta_2} \in [0,1]$ and $\beta_0 - \frac{|\beta_1|^2}{4\beta_2} \leq 0$, *i.e.* β s.t. $\beta_2 < -\frac{|\beta_1|}{2}$ and $\beta_0 \leq \frac{|\beta_1|^2}{4\beta_2}$, this is equivalent to saying that for all $\beta_2 < -\frac{|\beta_1|}{2}$, we have:

$$\frac{|\beta_1|^2}{4\beta_2} M_0 + |\beta_1||M_1| + \beta_2 M_2 \leq 0.$$

For a fixed β_2 s.t. $\beta_2 \leq -\frac{|\beta_1|}{2}$, consider the function $G : \mathbb{R} \to \mathbb{R}$ such that:

$$G(|\beta_1|) = |\beta_1|^2 M_0 + 4\beta_2 |\beta_1||M_1| + 4\beta_2^2 M_2.$$

For the function G to be positive (because $\beta \geq 0$), it is necessary and sufficient that its minimum is positive. As $G(0) \geq 0$ and $G(+\infty) = +\infty$, this minimum is reached at a finite value of $|\overline{\beta_1}| \geq 0$. If $|\overline{\beta_1}| = 0$, then:

$$G'(|\beta_1|) = 2|\beta_1| M_0 + 4\beta_2 |\beta_1||M_1| \geq 0,\ \forall |\beta_1| > 0.$$

By passing to the limit $|\beta_1| \to 0$, we obtain $\beta_2 \geq 0$ which is a contradiction. Then $|\overline{\beta_1}| > 0$ and therefore $G'(|\overline{\beta_1}|) = 0$. This gives:

$$|\overline{\beta_1}| = -\frac{2\beta_2 |M_1|}{M_0}, \quad \text{and } \ G(|\overline{\beta_1}|) = \frac{4\beta_2^2}{M_0}(M_2 M_0 - |M_1|^2).$$

The necessary and sufficient condition is $G(|\overline{\beta_1}|) \geq 0$ which is equivalent to: $M_2 M_0 - |M_1|^2 \geq 0$.

Let us consider now β s.t. $\beta_0 \leq 0$ and $\beta_0 + |\beta_1| + \beta_2 \leq 0$ and $-\frac{|\beta_1|}{2\beta_2} \notin [0,1]$. Combining the three inequalities, we obtain: $\beta_0 \leq -(|\beta_1| + \beta_2)$ and $\beta_2 > -\frac{|\beta_1|}{2}$. Recall that we must prove, for all these β :

$$\beta_0 M_0 + |\beta_1||M_1| + \beta_2 M_2 \leq 0.$$

Thanks to $\beta_0 \leq -(|\beta_1| + \beta_2)$, this is equivalent to saying that for all $\beta_2 > -\frac{|\beta_1|}{2}$, we have:

$$|\beta_1|(|M_1| - M_0) + \beta_2(M_2 - M_0) \leq 0.$$

By passing to the limit $|\beta_1|$ and $\beta_2 \to +\infty$, we obtain the following conditions:

$$M_2 \leq M_0 \quad \text{and} \quad |M_1| \leq M_0.$$

Moreover, the inequality $|\beta_1|(|M_1| - M_0) + \beta_2(M_2 - M_0) \leq 0$ is satisfied $\forall \beta_2$ s.t. $\beta_2 > -\frac{|\beta_1|}{2}$. So, it follows that $M_0 - 2|M_1| + M_2 \geq 0$.

Finally, the necessary and sufficient conditions on (M_0, M_1, M_2) reads:

$$M_2 \leq M_0, \ |M_1|^2 \leq M_0 M_2, \ M_0 - 2|M_1| + M_2 \geq 0, \quad \text{and } |M_1| \leq M_0.$$

We can easily show that the first two conditions imply the last two ones. Therefore, the moment problem (5.1) admits a solution in D if and only if:

$$2W_1 - 2\underline{u} \cdot P_1 + n_1|\underline{u}|^2 \leq \mathcal{R}^2 \underline{T} n_1, \qquad |P_1|^2 \leq 2W_1 n_1.$$

□

5.2 Appendix B: Calculations relative to the proof of proposition 2.4:

In this section, we prove that expression (2.15) can be simplified. Indeed, the volumic terms preceded by the minus sign in (2.15) vanish. More precisely, we show that:

$$\frac{\partial}{\partial t}\left(\tilde{m}(w)J\right) + \nabla_x \cdot \left((\mathcal{R}\sqrt{\underline{T}}w + \underline{u})\tilde{m}(w)J\right) + \nabla_w \cdot \left(\tilde{m}(w)\overrightarrow{F_1}(w)J\right) = 0, \tag{5.1}$$

where $\tilde{m}(w)$ is the vector of the conserved quantities in the w variable:

$$\tilde{m}(w) = \begin{pmatrix} 1 \\ \mathcal{R}\sqrt{\underline{T}}w + \underline{u} \\ |\mathcal{R}\sqrt{\underline{T}}w + \underline{u}|^2 \end{pmatrix},$$

J is the Jacobian $J = (\mathcal{R}\sqrt{\underline{T}})^d$, $d = 1, 2, 3$, and $\overrightarrow{F_1}(w)$ is the force term given by (2.16). Let us calculate the divergence of this force term:

$$\nabla_w \cdot \overrightarrow{F_1}(w) = -\frac{1}{\mathcal{R}\sqrt{\underline{T}}}\left[\mathcal{R}\sqrt{\underline{T}}\nabla_x \cdot \underline{u} + d\left(\frac{\partial}{\partial t} + (\underline{u} + \mathcal{R}\sqrt{\underline{T}}w) \cdot \nabla_x\right)\mathcal{R}\sqrt{\underline{T}} + \mathcal{R}\sqrt{\underline{T}}w \cdot \nabla_x(\mathcal{R}\sqrt{\underline{T}})\right] \tag{5.2}$$

Now, we investigate the mass component, *i.e.* when $\tilde{m}(w) = 1$. In this case, (5.1) is written:

$$\frac{\partial J}{\partial t} + \nabla_x \cdot \left((\mathcal{R}\sqrt{\underline{T}}w + \underline{u})J\right) + \nabla_w \cdot \left(\overrightarrow{F_1}(w)J\right)$$
$$= d\frac{\partial \mathcal{R}\sqrt{\underline{T}}}{\partial t}\left(\mathcal{R}\sqrt{\underline{T}}\right)^{d-1} + J\nabla_x \cdot \left(\mathcal{R}\sqrt{\underline{T}}w + \underline{u}\right)$$
$$+d\left(\mathcal{R}\sqrt{\underline{T}}w + \underline{u}\right) \cdot \nabla_x(\mathcal{R}\sqrt{\underline{T}})\left(\mathcal{R}\sqrt{\underline{T}}\right)^{d-1} + J\nabla_w \cdot \left(\overrightarrow{F_1}(w)\right).$$

Thanks to the expression (5.2), this term is equal to zero.

The momentum component corresponds to $\tilde{m}(w) = \mathcal{R}\sqrt{\underline{T}}w + \underline{u}$. Let us detail the calculations of the three terms of (5.1). The first one gives,

$$\frac{\partial}{\partial t}(\tilde{m}(w)J) = J\left(\frac{\partial \tilde{m}(w)}{\partial t}\right) + d\left(\underline{u} + \mathcal{R}\sqrt{\underline{T}}w\right)\frac{\partial \mathcal{R}\sqrt{\underline{T}}}{\partial t}(\mathcal{R}\sqrt{\underline{T}})^{d-1},$$

whereas the second one becomes, (with $\tilde{m}(w) = \underline{u} + \mathcal{R}\sqrt{\underline{T}}$):

$$\nabla_x \cdot (\tilde{m}(w)\tilde{m}(w)J) = (\tilde{m}(w)\tilde{m}(w) \cdot \nabla_x)\, J + J\left[(\nabla_x \cdot \tilde{m}(w))\,\tilde{m}(w) + (\nabla_x \tilde{m}(w))\,\tilde{m}(w)\right]$$

Finally, the last term can be written as follows:

$$\nabla_w \cdot \left(\tilde{m}(w)\overrightarrow{F}_1(w)J\right) = J\left(\nabla_w \tilde{m}(w)\right)\overrightarrow{F}_1(w) + J\left(\nabla_w \cdot \overrightarrow{F}_1(w)\right)\tilde{m}(w).$$

If we use (5.2) in the last term, we find:

$$\nabla_w \cdot \left(\tilde{m}(w)\overrightarrow{F}_1(w)J\right)$$
$$= J\mathcal{R}\sqrt{\underline{T}}\overrightarrow{F}_1(w)$$
$$-\frac{J}{\mathcal{R}\sqrt{\underline{T}}}\left[\mathcal{R}\sqrt{\underline{T}}\nabla_x \cdot \underline{u} + d\left(\frac{\partial}{\partial t} + (\underline{u} + \mathcal{R}\sqrt{\underline{T}}w) \cdot \nabla_x\right)\mathcal{R}\sqrt{\underline{T}} + \mathcal{R}\sqrt{\underline{T}}w \cdot \nabla_x(\mathcal{R}\sqrt{\underline{T}})\right]\tilde{m}(w)$$
$$= -J\left[\left(\frac{\partial}{\partial t} + (\underline{u} + \mathcal{R}\sqrt{\underline{T}}w) \cdot \nabla_x\right)(\underline{u} + \mathcal{R}\sqrt{\underline{T}}w)\right]$$
$$-\frac{J}{\mathcal{R}\sqrt{\underline{T}}}\left[\mathcal{R}\sqrt{\underline{T}}\nabla_x \cdot \underline{u} + d\left(\frac{\partial}{\partial t} + (\underline{u} + \mathcal{R}\sqrt{\underline{T}}w) \cdot \nabla_x\right)\mathcal{R}\sqrt{\underline{T}} + \mathcal{R}\sqrt{\underline{T}}w \cdot \nabla_x(\mathcal{R}\sqrt{\underline{T}})\right]\tilde{m}(w).$$

If we develop and sum these three terms, we can see that they vanish.

Finally, let us calculate the third component (the energy component). In this case, $\tilde{m}(w)$ is equal to $\left|\underline{u} + \mathcal{R}\sqrt{\underline{T}}\right|^2$. We then denote $\left|\underline{u} + \mathcal{R}\sqrt{\underline{T}}\right|^2$ by $\tilde{m}(w)$. As in the momentum calculations, we investigate each of the three terms of (5.1). For the first term, we have:

$$\frac{\partial}{\partial t}\left(J\tilde{m}(w)\right) = 2J\frac{\partial(\underline{u} + \mathcal{R}\sqrt{\underline{T}})}{\partial t} \cdot (\underline{u} + \mathcal{R}\sqrt{\underline{T}}) + d\tilde{m}(w)\frac{\partial(\mathcal{R}\sqrt{\underline{T}})}{\partial t}(\mathcal{R}\sqrt{\underline{T}})^{d-1},$$

and for the second term of (5.1), where $\tilde{m}(w) = \left|\underline{u} + \mathcal{R}\sqrt{\underline{T}}\right|^2$, we find:

$$\nabla_x \cdot \left((\underline{u} + \mathcal{R}\sqrt{\underline{T}})\tilde{m}(w)J\right)$$
$$= \tilde{m}(w)J\nabla_x \cdot (\underline{u} + \mathcal{R}\sqrt{\underline{T}}) + J(\underline{u} + \mathcal{R}\sqrt{\underline{T}}) \cdot \nabla_x \tilde{m}(w) + \tilde{m}(w)(\underline{u} + \mathcal{R}\sqrt{\underline{T}}) \cdot \nabla_x J.$$

Finally, the third term of (5.1) can be developed as follows:

$$
\begin{aligned}
&\nabla_w \cdot \left(\tilde{m}(w)\overrightarrow{F}(w)J\right) \\
&\quad = J\tilde{m}(w)\nabla_w \cdot \overrightarrow{F}(w) + J\overrightarrow{F}(w)\cdot\nabla_w\tilde{m}(w) \\
&\quad = -\frac{J\tilde{m}(w)}{\mathcal{R}\sqrt{\underline{T}}}\left[\mathcal{R}\sqrt{\underline{T}}\nabla_x\cdot\underline{u} + d\left(\frac{\partial}{\partial t} + (\underline{u}+\mathcal{R}\sqrt{\underline{T}}w)\cdot\nabla_x\right)\mathcal{R}\sqrt{\underline{T}} + \mathcal{R}\sqrt{\underline{T}}w\cdot\nabla_x(\mathcal{R}\sqrt{\underline{T}})\right] \\
&\qquad -\frac{2J}{\mathcal{R}\sqrt{\underline{T}}}\left[\left(\frac{\partial}{\partial t} + (\underline{u}+\mathcal{R}\sqrt{\underline{T}}w)\cdot\nabla_x\right)(\underline{u}+\mathcal{R}\sqrt{\underline{T}}w)\right]\cdot(\underline{u}+\mathcal{R}\sqrt{\underline{T}}w)\mathcal{R}\sqrt{\underline{T}} \\
&\quad = -\frac{J\tilde{m}(w)}{\mathcal{R}\sqrt{\underline{T}}}\left[\mathcal{R}\sqrt{\underline{T}}\nabla_x\cdot\underline{u} + d\frac{\partial\mathcal{R}\sqrt{\underline{T}}}{\partial t} + (\underline{u}+\mathcal{R}\sqrt{\underline{T}}w)\cdot\nabla_x\mathcal{R}\sqrt{\underline{T}} + \mathcal{R}\sqrt{\underline{T}}w\cdot\nabla_x(\mathcal{R}\sqrt{\underline{T}})\right] \\
&\qquad -2J\left[\frac{\partial(\underline{u}+\mathcal{R}\sqrt{\underline{T}}w)}{\partial t}\cdot(\underline{u}+\mathcal{R}\sqrt{\underline{T}}w)\right] \\
&\qquad -2J\left[\left((\underline{u}+\mathcal{R}\sqrt{\underline{T}}w)\cdot\nabla_x(\underline{u}+\mathcal{R}\sqrt{\underline{T}}w)\right)\cdot(\underline{u}+\mathcal{R}\sqrt{\underline{T}}w)\right]
\end{aligned}
$$

The sum of these three terms vanish. We conclude that (5.1) vanishes.

5.3 Appendix C: Numerical resolution of discrete moment and entropy problems:

As in the continuous case, the discrete entropy minimization problem requires the resolution of a discrete moment problem. First, for numerical reasons, we must restrict the discrete velocity space $\mathbb{Z}$ to a finite discrete set. Let $\mathcal{K}$ be the following set of indices:

$$\mathcal{K} = \{k \in \mathbb{N} \text{ such that } k \leq 2K\}, \tag{5.1}$$

where $K > 0$ is given. We then define a discrete velocity set $\mathcal{V}$ of $\mathbb{R}$ by:

$$\mathcal{V} = \{v_k = (k-K)\Delta v, k \in \mathcal{K}\},$$

where Δv is the velocity step, $\Delta v > 0$. Three minimization problems take place in our scheme: (3.2), (3.8) and, in the second step of the algorithm, (3.8) with prescribed moments $\tilde{U}_{1,i}^{n+1}$. The first one (3.2) determines $\mathcal{E}_{i,k}^n$. At the continuous level, we have seen that $\mathcal{E}_{i,k}^n$ has an exponential form (2.5). At the discrete level, we use a result of [22] stating that this property remains true provided that the set (5.1) contains at least three points (which is not very restrictive) and the prescribed discrete moments U_i^n are strictly realizable, *i.e.* U_i^n is the moment vector of a strictly positive discrete function (which is fulfilled thanks to proposition 3.1 and remark 3.2). Consequently, thanks to this result, we let:

$$\mathcal{E}_{i,k}^n = \exp(\alpha_i^n \cdot m_k), \quad \forall k \in \mathcal{K}.$$

So, it is sufficient to solve the following discrete moment problem:

$$\left\{\begin{array}{l} \text{Find } \alpha_i^n \in \mathbb{R}^3 \text{ such that for } U_i^n \in \mathbb{R}^3 \text{ given} \\ \displaystyle\sum_{k\in\mathcal{K}} \exp(\alpha_i^n \cdot m_k) = U_i^n. \end{array}\right. \tag{5.2}$$

As well as for (3.8), if $\mathcal{K}_i^n$ contains more than three points and the prescribed discrete moments $U_{1,i}^n$ are strictly realizable (which is satisfied thanks to proposition 3.1 and remark 3.2), the second minimization problem (3.8) yealds $\mathcal{M}_{1,i,k}^n$ which also has an exponential form:

$$\mathcal{M}_{1,i,k}^n = \exp(\lambda_{1,i}^n \cdot m_k), \ \ \forall k \in \mathcal{K}_i^n.$$

So, we only have to solve the following discrete moment problem:

$$\left\{ \begin{array}{l} \text{Find } \lambda_{1,i}^n \in \mathbb{R}^3 \text{ such that for } U_{1,i}^n \in \mathbb{R}^3 \text{ given} \\ \displaystyle\sum_{k \in \mathcal{K}_i^n} \exp(\lambda_{1,i}^n \cdot m_k) = U_{1,i}^n. \end{array} \right. \tag{5.3}$$

Let us now pay attention to the resolution of the third minimization problem (3.8) with prescribed moments $\tilde{U}_{1,i}^{n+1}$. It allows us to obtain $\tilde{\mathcal{M}}_{1,i,k}^{n+1}$, $\forall k \in \mathcal{K}_i^n$ in the second step of the algorithm. We have to solve (3.8) with prescribed moments $\tilde{U}_{1,i}^{n+1}$. Nevertheless, we do not know if the prescribed moments $\tilde{U}_{1,i}^{n+1}$ are satisfied by a strictly positive discrete distribution. So, we can not apply the result of [22]. The problem is different and we are faced with a discrete moment realizability problem; we are seeking conditions on $\tilde{U}_{1,i}^{n+1}$ so that there exists a strictly positive discrete distribution, the moments of which should be equal to $\tilde{U}_{1,i}^{n+1}$. However, the restriction on the time step ensures that $\tilde{U}_{1,i}^{n+1}$ is not "far" from $U_{1,i}^n$ which is strictly realizable; consequently, in practice, we solve this entropy minimization problem in the same way as the two previous entropy minimization problems, *i.e.* solving the discrete associated moment problem:

$$\left\{ \begin{array}{l} \text{Find } \tilde{\lambda}_{1,i}^{n+1} \in \mathbb{R}^3 \text{ such that for } \tilde{U}_{1,i}^{n+1} \in \mathbb{R}^3 \text{ given} \\ \displaystyle\sum_{k \in \mathcal{K}_i^n} \exp(\tilde{\lambda}_{1,i}^{n+1} \cdot m_k) = \tilde{U}_{1,i}^{n+1}. \end{array} \right. \tag{5.4}$$

Consequently, the computation of these three discrete entropy minimization problems does not require the resolution of some expensive minimization problems. Indeed, it is sufficient to solve the associated discrete moment problems (5.2), (5.3) and (5.4).

Let us now consider the numerical resolution of the discrete moment problems (5.2), (5.3) and (5.4). Several strategies can be used to solve them (see [24] or [22]). We have chosen here a Newton algorithm.

Acknowledgements: Support by the Commissariat à l'énergie atomique (LRC MIP-CEA M06) and by the European network HYKE (EC contract HPRN-CT-2002-00282), is aknowledged. The authors wish to thank B. Dubroca and J.P. Morreuw for stimulating discussions and encouragements.

References

[1] A.M. Anile, V. Romano, G. Russo, *Extended hydrodynamical model of carrier transport in semiconductors*, SIAM J. APPL. Math., **61**, (2000), n1, 74-101.

[2] K. Aoki, K. Kanba, S. Takata, *Numerical analysis of a supersonic rarefied gas flow past a flat plate*, Phys. Fluids, Vol. **9** (4), pp. 1144-1161, 1997.

[3] P.L. Bathnagar, E.P. Gross, M. Krook, *A model for collision processes in gases. I. small amplitude processes in charged and neutral one-component systems*, Phys. Rev., 94:511-525, 1954.

[4] G.A. Bird, *Molecular gas dynamics and the direct simulation of gas flows*, Oxford Science Publications, 1994.

[5] J.F. Bourgat, P. Le Tallec, B. Perthame, Y. Qiu, *Coupling Boltzmann and Euler equations without overlapping,* Domain Decomposition Methods in Science and Engineering (COMO, 1992), 377-398, Amer. Math. Soc..

[6] S. Brunner, E. Valeo, J.A. Krommes, *Linear delta-f simulations of nonlocal electron heat transport*, Phys. Plasmas, Vol. 7, No. 7, July 2000.

[7] C. Buet, *A discrete-velocity scheme for the Boltzmann operator of rarefied gas dynamics*, Transp. Th. Stat. Phys. **25**(1), 33-60 (1996).

[8] C. Cercignani, *The Boltzmann Equation and Its Applications*, volume 68, Springer-Verlag, Lectures Series in Mathematics, 1988.

[9] S. Chapman, T.G. Cowling, *The Mathematical Theory of Non-Uniform Gases*, Cambridge University Press, 1970.

[10] N. Crouseilles, *Dérivation de modèles couplés dérive-diffusion/cinétique par une méthode de décomposition en vitesse*, C. R. Acad. Sci. Paris, Ser. I 334 (2002), 827-832.

[11] N. Crouseilles, P. Degond, M. Lemou, *Hybrid kinetic/fluid models for nonequilibrium systems*, C. R. Acad. Sci. Paris, Ser. I 336 (2003).

[12] P. Degond, M. Lemou, *Turbulence models for incompressible fluids derived from kinetic theory*, J. Math. Fluid Mech. 4 (2002), 257-284.

[13] P. Degond, P.F. Peyrard, G.Russo, Ph. Villedieu, *Polynomial upwind schemes for hyperbolic systems*, C. R. Acad. Sci. Paris, Série 1, 328, p.479-483, 1999.

[14] B. Dubroca, A. Klar, *Prise en compte d'un fort déséquilibre cinétique par un modèle aux demi-moments*, C.R. Math. Acad. Sci. Paris, **335** (2002), n 8, 699-704.

[15] D. Goldstein, B. Sturtevant and J.E. Broadwell, *Investigations of the motion of discrete-velocity gases*, Rarefied Gas Dynamics, (1989).

[16] H. Grad, *On the kinetic theory of rarefied gases*, Commun. Pure Appl. Math 2, 1949.

[17] H. Grad, *Principles of the kinetic theory of gases*, in Flugge S. (Ed.), Handbuch der Physik, Vol. XII, Springer, Berlin, 1958.

[18] F. Gropengiesser, H. Neunzert, J. Struckmeier, B. Wiesen, *Rarefied gas flow around a disc with different angles of attack*, Rarefied Gas Dynamics, p 546-553, VCH, Weinheim, 1991.

[19] C. Groth, T.I. Gombosi, P. Roe, S. Brown, *Gaussian-based moment-method closures for the solution of the Boltzmann equation*, Hyperbolic problems: theory, numerics, applications (Stony Brook, NY, 1994), 339-346, World Sci. Publishing, 19961.

[20] M. Junk, *Maximum entropy for reduced moment problem*, Math. Models and Meth. in Applied Sc., Vol. 10, **7**, pp. 1001-1025.

[21] C.D. Levermore, *Moment closure hierarchies for kinetic theories*, J. Stat. Phys., **83** (1996), pp. 1021-1065.

[22] L. Mieussens, *Discrete velocities model and implicit scheme for the BGK equation of rarefied gas dynamics*, Math. Models and Meth. in Applied Sc., Vol. 10, **8**, pp. 1121-1149.

[23] P. Le Tallec, F. Mallinger, *Coupling Boltzmann and Navier-Stokes equations by half fluxes*, J. Comput. Phys., **136** (1997), n1, pp. 51-67.

[24] P. Le Tallec, J.P. Perlat, *Coupling kinetic models with Navier-Stokes equations*, CFD Review, Vol II, 833-855, 1998.

[25] I. Muller, T. Ruggeri, *Rational extended thermodynamics*, Springer Tracts in Natural Philosophy, volume 37, Second edition, 1998.

[26] K. Nanbu, *Direct simulation scheme derived from the Boltzmann equation*, J. Phys. Soc. of Japan, 45:2042-2049, 1980.

[27] S.E. Parker, W.W. Lee, *A fully nonlinear characteristic method for gyrokinetic simulation*, Phys. Fluids, Vol. B **5**, pp. 77-86, 1993.

[28] J.P. Perlat, *Modélisation et calcul parallèle d'une couche limite cinétique*, PhD thesis, Université Pierre et Marie Curie, Paris 6, (1997).

[29] F. Rogier, J. Schneider, *A direct method for solving the Boltzmann equation*, Transp. Th. Stat. Phys., 23(1-3):313-338, 1994.

[30] G.A. Sod, *A survey of several finite difference methods for systems of nonlinear hyperbolic conservation laws*, J. Comput. Phys., **27**(1), pp. 1-31, (1978).

[31] H.C. Yee, *A class of high-resolution explicit and implicit shock-capturing methods*, Von Karman Institute for Fluid Dynamics, Lecture Series, Vol.4, 1989.